Department of Engineering Physics and Mathematics
Laboratory of Biomedical Engineering
Helsinki University of Technology
Espoo, Finland

Cardiac exercise studies with bioelectromagnetic mapping

Panu Takala

Dissertation for the degree of Doctor of Science in Technology to be presented with due permission for public examination and debate in Auditorium F1 at Helsinki University of Technology (Espoo, Finland) on the 17th of November, 2001, at 12 o'clock noon.

Espoo 2001

ISBN 951-22-5719-X

Abstract

Bioelectric currents in the heart give rise to differences in electric potential in the body and on its surface. The currents also induce a magnetic field within and outside the thorax. Recording of the electric potential on the surface of the body, electrocardiography (ECG), is a well established clinical tool for detecting insufficient perfusion of blood, i.e., ischemia during exercise testing. In a more recent technique, magnetocardiography (MCG), the cardiac magnetic field is recorded in the vicinity of the chest. Despite the clinical significance of the exercise ECG recordings in patients with suspected coronary artery disease (CAD), little is known about the effect of stress in the MCG of healthy subjects and patients with CAD.

Methods for analysing multichannel MCG signals, recorded during physical exercise testing, were developed in this thesis. They were applied to data recorded in healthy subjects to clarify the normal response to exercise in the MCG, and to data of patients with CAD to detect exercise-induced myocardial ischemia. Together with the MCG, spatially extensive ECG, i.e., body surface potential mapping (BSPM) was studied and the exercise-induced alterations in the two mappings were compared.

In healthy volunteers, exercise was found to induce more extensive alterations in the MCG than in the BSPM during the ventricular repolarisation. In patients with CAD, when optimal recording locations were found and evaluated, alterations of the ST segment in the MCG could be used as indicators of ischemia. Also, ischemia was found to induce a rotation of magnetic field maps (MFMs) which illustrate the spatial MCG signal distribution. The MFM orientation could successfully be used as a parameter for ischemia detection. In the BSPM, regions sensitive to ischemia-induced ST segment depression, ST segment elevation, and ST segment slope decrease were identified.

An analysis method was also developed for monitoring the development of the MCG and the BSPM distributions. It enables examination of different features of the MCG and the BSPM signals as a function of time or the heart rate. In this thesis, the method was used for quantifying exercise-induced change in the orientation of MFMs. Adjustment of the orientation change with the corresponding alteration of the heart rate was found to improve ischemia detection by the exercise MCG. When data recorded during the recovery period of exercise testing were evaluated with similar type of analysis methods, the MCG showed better performance in ischemia detection than the simultanously recorded 12-lead ECG.

Contents

List of Publications

This thesis consists of an overview and of the following six publications:

I Takala P, Hänninen H, Montonen J, Mäkijärvi M, Nenonen J, Oikarinen L, Simelius K, Toivonen L and Katila T "Magnetocardiographic and electrocardiographic exercise mapping in healthy subjects" *Ann. Biomed. Eng.* **29** 501–9 (2001).

II Hänninen H, Takala P, Mäkijärvi M, Montonen J, Korhonen P, Oikarinen L, Nenonen J, Katila T and Toivonen L "Detection of exercise induced myocardial ischemia by multichannel magnetocardiography in single vessel coronary artery disease" *Ann. Noninv. Electrocardiology* **5** 147–57 (2000).

III Hänninen H, Takala P, Mäkijärvi M, Montonen J, Korhonen P, Oikarinen L, Simelius K, Nenonen J, Katila T and Toivonen L "Recording locations in multichannel magnetocardiography and body surface potential mapping sensitive for regional exercise-induced myocardial ischemia" *Basic Res. Cardiol.* **96** 405–14 (2001).

IV Takala P, Hänninen H, Montonen J, Mäkijärvi M, Nenonen J, Toivonen L and Katila T "Beat-to-beat analysis method for magnetocardiographic recordings during interventions" *Phys. Med. Biol.* **46** 975–82 (2001).

V Takala P, Hänninen H, Montonen J, Korhonen P, Mäkijärvi M, Nenonen J, Oikarinen L, Toivonen L and Katila T "Heart rate adjustment of magnetic field map rotation in detection of myocardial ischemia in exercise magnetocardiography" *Basic Res. Cardiol.* Accepted for publication (2001).

VI Hänninen H, Takala P, Mäkijärvi M, Korhonen P, Oikarinen L, Simelius K, Nenonen J, Katila T and Toivonen L "ST segment level and slope in exercise-induced myocardial ischemia evaluated with body surface potential mapping" *Am. J. Cardiol.* Accepted for publication (2001).

List of abbreviations

The most important abbreviations used in the overview are listed and shortly explained below.

AUC	area under curve
bpm	beats per minute
BSPM	body surface potential mapping / map
CAD	coronary artery disease
CDE	current density estimate
dc	direct current
DI	discriminant index
ECD	equivalent current dipole
ECG	electrocardiography / -graphic
HR	heart rate
HUCH	Helsinki University Central Hospital
HUT	Helsinki University of Technology
LAD	left anterior descending coronary artery
LCX	left circumflex coronary artery
MCG	magnetocardiography / -graphic
MFM	magnetic field map
MI	myocardial infarct
MRI	magnetic resonance imaging
RCA	right coronary artery
ROC	receiver operator characteristic
SD	standard deviation
SI	smoothness index
SQUID	superconducting quantum interference device

1 Introduction

Bioelectric currents in the heart give rise to differences in electric potential in the body and on its surface. The same currents induce also a magnetic field within and outside the thorax. The recording of electric potential differences on the body surface is called electrocardiography (ECG). In magnetocardiography (MCG), the magnetic field is measured in the vicinity of the chest. The ECG and the MCG provide non-invasive means for studying the cardiac function and diseases of the heart.

In coronary artery disease (CAD), the blood flow and oxygen delivery to the heart are hampered by a stenosis in one or several coronary arteries. If the stenosis results in insufficient perfusion, i.e. ischemia, it may depress the function of the myocardial area nourished by the culprit vessel. Ischemia may also alter the electric activation of the heart, which forms the basis for diagnosis of CAD by the ECG and the MCG. In many cases ischemia occurs only when the demand for blood in the heart is increased by physical or mental stress. Electrophysiological effects of ischemia are discussed in section 2 of this thesis.

The most widely used diagnostic and prognostic test for CAD is 12-lead exercise ECG, in which physical exercise is used to provoke ischemia. It is inexpensive, fast and well-standardized test but its sensitivity to CAD is less than 75% (Gianrossi *et al.* 1989). In women, the accuracy of standard exercise ECG is impaired by increased rate of false positive findings (Alexander *et al.* 1998). Other non-invasive methods for detecting ischemia are therefore demanded. The MCG has been suggested to provide information complementary to the ECG on the cardiac function (Brockmeier *et al.* 1994 and 1997, Lant *et al.* 1990). Compared to the ECG, the MCG is a recent technique. The first commercial multichannel MCG devices became available in the beginning of the 1990's (Nowak 1998). The recording of multichannel MCG during exercise testing provides an extensive spatial scope and good temporal resolution for studying the heart in changing physiological conditions. However, lack of commercially available non-magnetic exercise equipment and low number of multichannel MCG recording devices have stalled the research on the exercise MCG. The methods and main results of previous stress MCG studies are described in section 3 of this thesis.

In this thesis, new methods for recording and analysing multichannel exercise MCG data were developed. The aims were to clarify the response of healthy subjects to exercise in the MCG, and to develop methods for detecting ischemia by exercise MCG in patients with CAD. Together with the MCG, the spatially extensive electric body surface potential mapping (BSPM) was studied, and these two noninvasive mapping methods were compared.

A laboratory-made non-magnetic ergometer (Takala 1997) that enabled the exercise MCG recordings, was used in this study. The ergometer and the exercise MCG measurement protocol used in this thesis are described in the latter part of section 3.

A multichannel exercise MCG recording provides a multitude of spatial and temporal

information. Effective signal processing is therefore essential for rejecting artefacts, improving the signal to noise ratio, and extracting and quantifying the desired features in the signal. Signal analysis methods used in previous studies and those developed in this thesis are presented in section 4.

Main results of the studies on patients and healthy controls, obtained in this thesis, are described in section 5. The effect of exercise on the MCG and the BSPM signals of healthy subjects was evaluated and the two mappings were compared in Publication I. In Publication II, ischemia-induced changes in the MCG were quantified and a method for detecting ischemia in CAD patients by the MCG was developed. The optimal recording locations for detecting CAD by the MCG and the ECG were studied in Publication III. Utilising a beat-to-beat analysis method developed in Publication IV, ischemia detection by heart rate adjustment of alteration in the MCG was studied in Publication V. In Publication VI, optimal recording locations for detecting exercise-induced ischemia by signal amplitude and morphology in the BSPM were studied in a heterogeneous CAD patient population. The methods and results of this thesis are discussed in section 6.

2 Electrophysiological effects of myocardial ischemia

2.1 Genesis of normal ventricular action potential

The ECG and MCG signals are caused by electric activation of cardiac cells. This activity is to a large extent determined by the active and passive properties of the cell membrane which regulates the flux of ions in and out of the cell. Normally, the electrically active cells of ventricular myocardium have a resting membrane potential of approximately -78 mV (Surawicz 1995). This potential is mainly generated by the concentration gradients of sodium (Na^+) and potassium (K^+) ions over the cell membrane. The ratio of intracellular to extracellular K^+ concentration is approximately 30:1 and the corresponding ratio of Na^+ is 1:15. The equilibrium potential, determined by the Nernst equation, is -94 mV for K^+ and +41 mV for Na^+. At rest the cell membrane is nearly freely permeable to K^+ but not very permeable to Na^+. Thereby, the membrane potential is close to the equilibrium potential of K^+.

The depolarisation of a cardiac cell consists of a fast change of the membrane potential from a steady state close to the equilibrium potential of Na^+. It is determined almost exclusively by an increase in Na^+ conductance as a function of membrane potential. The depolarisation is initiated by a propagating electric impulse, causing an increase of the membrane potential to the threshold of about -55 to -50 mV. Consequently, the permeability of Na^+ ions increases allowing influx of Na^+ ions. This increases the intracellular concentration of cations and further depolarisation takes place. Depolarisation continues until the membrane potential becomes close to the resting membrane potential of Na^+. In ventricular cells the depolarisation is followed by a plateau of membrane potential during which a balance between inward and outward currents through the membrane is maintained. Repolarisation back to the resting membrane potential is nearly 100 times slower than the depolarisation. It is primarily due to passive influx of K^+ ions to the cell, bringing the membrane potential close to the equilibrium potential of K^+. The concentration gradients of Na^+ and K^+ ions and the resting membrane potential are maintained by active, energy-consuming Na^+/K^+ pumps.

The electrical activation induces mechanical contraction of the cardiac cell. The contraction is initiated by an influx of Ca^{2+} ions to the cell during the plateau of the action potential. During the activation the cell is refractory and does not respond to additional electric stimulus. In the ECG and MCG signal morphology, the QRS complex originates from the depolarisation of ventricular myocardium, the ST segment corresponds to the plateau of the action potential, and the T wave corresponds to the repolarisation phase of ventricular myocardium (Fig. 1).

2.2 Effects of myocardial ischemia

2.2.1 Changes in ventricular action potential and electrocardiogram

Myocardial ischemia depolarises of the resting membrane potential toward the zero potential and decreases the upstroke velocity of the action potential. It also results in shorter duration and lower amplitude of action potential (Fig. 1). The processes behind these alterations are diverse, the major contributors being cellular potassium loss, accumulation of extracellular K^+, and acidosis (Surawicz 1995). In exercise-induced ischemia in general, the alterations of action potential take place first at the subendocardium.

During the plateau of the ventricular action potential, corresponding to the ST segment of the ECG, the intracellular potential of the healthy myocardial cells is higher than the potential of the ischemic cells. This induces the systolic injury current form the healthy to the ischemic myocardium and larger positive charge densities on the membrane surfaces of the ischemic cells (Savard 1983). Correspondingly, the negative charge density is higher on the membrane surfaces on the healthy cells and a depression of the ST segment is seen in the precordial ECG leads. The alterations in the action potential and the systolic injury current are illustrated in Fig. 1.

Different resting membrane potentials of the healthy and the ischemic myocardium induce a diastolic injury current. During the TP interval in the ECG, the intracellular potential is higher in the ischemic cells than in the normal cells. The injury current flows from the ischemic toward the normal tissue and the positive charge density is higher on the membrane surfaces of the normal cells (Savard 1983). This diastolic current flows during the TP interval of the ECG and is interrupted during the ST segment. The more positive charge density on the membrane surfaces of the normal cells compared to ischemic cells induces an elevation of the baseline in the precordial ECG leads (Surawicz 1995). The conventional ECG, recorded with alternating current coupled amplifiers, does not reveal displacement of the baseline, and therefore does not differentiate between the ST segment displacement caused by the systolic and the diastolic injury current.

In the simplest model of the ischemia-induced current, the currents over the boundary of ischemic and normal myocardium are lumped into a single current dipole $\mathbf{p}$. In an infinite homogeneous and isotropic volume conductor, a current dipole induces an electric potential

$$V(\mathbf{r}) = \frac{1}{4\pi\sigma}\frac{\mathbf{p}\cdot\mathbf{R}}{R^3}, \tag{1}$$

where $\mathbf{r}$ is the observation point, $\mathbf{R}$ is the vector pointing from the location of the current dipole to $\mathbf{r}$, and σ is the conductivity of the medium. The dipole strength is proportional to the difference in membrane potentials of the normal and ischemic cells.

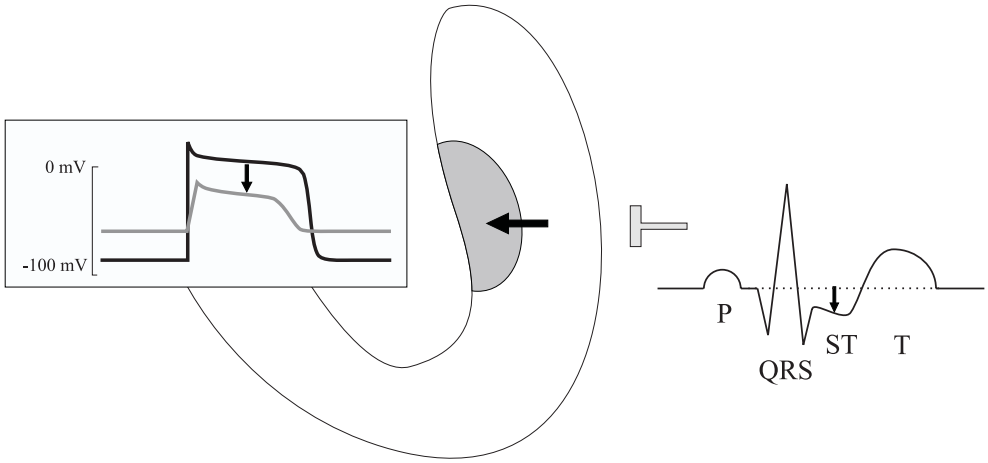

Fig. 1: *A schematic illustration of ischemia-induced changes of the myocardial action potential and the electrocardiogram (ECG). Left: the action potential of a normal (black curve) and an ischemic (grey curve) cell. Center: illustration of the left ventricle. Subendocardial ischemic myocardium is denoted by grey colour. Systolic injury current (black arrow) during the plateau of the action potential is directed from the healthy to the ischemic myocardium. Right: the subendocardial ischemia induces ST segment depression in the ECG leads at the left lateral thorax.*

2.2.2 Changes in magnetocardiogram

With the single current dipole source model and an infinite homogeneous and isotropic conductor, the ischemia-induced magnetic field can be expressed as

$$\mathbf{B}(\mathbf{r}) = \frac{\mu}{4\pi}\frac{\mathbf{p}\times\mathbf{R}}{R^3}, \tag{2}$$

where μ is the magnetic permeability of the medium. Thereby, an injury current in the heart oriented from the lower left chest toward the right shoulder would induce a magnetic field toward the upper left thorax and out of the central inferior chest during the ST segment.

The first-order approximations presented here are very rough. Both the ischemia-induced electric potential and magnetic field are affected by inhomogeneities and boundaries of the thorax, for example. Also, the ischemic current source is distributed and the dipole approximation is not optimal. Still, the simple current dipole model provides a means for making qualitative hypothesis for the ischemia-induced changes and their spatial distribution in the ECG and the MCG.

3 Magnetocardiographic stress studies

In spite of wide clinical use of exercise ECG, studies on stress MCG are few and patient populations are small. Current multichannel MCG devices are designed for studying a patient in a supine position. Thus, upright bicycle exercise or treadmill exercise, the standard protocols of exercise ECG, have not been available in multichannel MCG measurements. Also, the low amplitude of the cardiac magnetic field limits the use of magnetic materials in the exercise equipment.

Several methods have been used to induce stress in MCG recordings. The increase in heart rate by pharmacological stress is proportional to the dose of the drug. Because the subject does not move, it induces less noise in the MCG and ECG signals than physical stress. Dynamic physical exercise with a non-magnetic ergometer induces a substantial increase in the heart rate. It is also the natural way of exercise, can be stopped at any time, and compared to pharmacological stress it is easy to implement when the ergometer is available. Physical exercises of several types can be performed also further away from the measurement device before moving to the recording position. Such a protocol, however, prevents recording of data during exercise and immediately postexercise. Small elevation in the heart rate can also be evoked in the MCG measurements by mental stress or static physical stress (Takala *et al.* 2001).

In the following, a brief review is given on various stress methods and main results of previous studies. The signal processing methods of the studies are described in more detail in section 4. In the latter part of this section, the measurement equipment and protocol used in this work are described.

3.1 Review of the literature

The first exercise MCG recording was reported by Saarinen *et al.* (1974). They recorded single channel MCG in three precordial locations in healthy controls and in patients with various cardiac disorders. The study included also one patient with an old myocardial infarct (MI) and angina pectoris. In this patient, the post-exercise ST depressions were seen both in the ECG and the MCG. The authors found the ST-shift/R-wave amplitude ratio after exercise to be greater in the MCG than in the 12-lead ECG.

Cohen *et al.* (1976) recorded the MCG after exercise in one healthy volunteer in a magnetically shielded room. The exercise was induced by jogging in place for about ten minutes. The MCG was recorded postexercise in nine precordial locations with the subject in a standing position. A pronounced amount of ST segment depression was found in the MCG one minute after exercise but the separate exercise ECG recording showed only slight ST depression. The authors concluded that the MCG shows a greater ST depression than the ECG of comparable heart rate. In 1983 Cohen *et al.* reported direct-current (dc) MCG

measurements in a CAD patient undergoing two-step exercise test. Their aim was to study the mechanism underlying the ischemia-induced ST segment depression in the ECG. The recording was the first non-invasive measurement of injury current in the human heart. By recording the dcMCG they could separate the apparent (diastolic) and true (systolic) ST shifts and indicated the presence of the apparent type of ST shift. This shift is caused by injury current and is interrupted during the ST interval (see section 2). In recordings made at rest (Savard *et al.* 1983) in three patients with early repolarisation and in one patient with left bundle branch block they also studied the electrophysiological basis of the ST shift. They found that the ST shifts were not caused by a dc injury current. Instead, they were caused by a current flowing only during systole and the authors suggest that the ST shifts were due to altered repolarisation of the ventricles.

Brockmeier *et al.* (1994) studied 20 healthy young male subjects during exercise with single channel MCG. The MCG and unipolar ECG were recorded over a rectangular array of 16 precordial locations. The stress was induced with a wooden lever which the subject lifted with his legs. Using signal averaged data from all recording locations, the authors formed magnetic isofield maps (MFMs) illustrating the distribution of magnetic field component normal to the measurement plane. This work was the first MCG mapping study during exercise. Significant ST segment displacements were seen in the MCG but not in the ECG and the authors concluded that the MCG shows the junctional ST-T segment changes earlier than the ECG.

In the beginning of the 1990's the first multichannel MCG devices were constructed. For exercise studies this was a significant improvement, removing the need of continuous exercise at constant heart rate for acquiring data for one map. This promoted the clinical feasibility of exercise MCG mapping.

Kawaoka *et al.* (1996) used a non-magnetic stepper ergometer to induce mild stress during supine 37-channel MCG measurements in four normal subjects. They found a broad strong spatial correlation of adjacent channel measurements of atrial activity and changing correlation of more localised conduction system activity. Utilising these features they separated the atrial activity from conduction system activity and estimated conduction system changes during rest and exercise.

The first pharmacological stress MCG study was reported by Brockmeier *et al.* (1997). They induced pharmacological stress with atropine and orciprenaline during 37-channel MCG recordings in three healthy volunteers. In one subject also two reinvestigations were made. The ECG was recorded with 32 leads, simultaneously with the MCG. In concordance with their earlier work (Brockmeier *et al.* 1994) they found ST segment and T wave changes in the MCG, but not in the ECG. On some MCG channels, also T wave inversions took place during stress. The results are an important indication of difference between the ECG and the MCG. The authors suggest that the biophysical basis of this difference is the change

in the intensity and/or orientation of circular vortex currents.

Hailer *et al.* (1999) studied 15 patients with chest pain but no history of cardiovascular disease. Seven of the patients had a significant coronary stenosis, documented in coronary angiography. Pharmacological stress was induced by arbutamine during the 37-channel MCG measurements. The authors evaluated parameters based on spatial distribution of QT interval duration and found a significant difference between patients with and without significant coronary stenosis, both at rest and during stress. They concluded that evaluation of spatial distribution of QT interval duration increases the sensitivity of QT interval analysis in detection of CAD. They also suggested that complex repolarisation changes are not as apparent in 12-lead ECG as in MCG which has a better spatial scope.

Studies on stress MCG, published as long articles in referred journals before the year 2000, include a total of 22 subjects studied with a multichannel device. Twenty three subjects were studied with a single channel device. In addition, several conference abstracts and short papers on the topic have been published (Seese *et al.* 1995, Moshage *et al.* 1997, Gessner *et al.* 1999, Hänninen *et al.* 1999, Mäkijärvi *et al.* 1999, Pesola *et al.* 1999, Takala *et al.* 1999, Van Leeuwen *et al.* 1999 and 2001, Winklmaier *et al.* 1999, Fischer *et al.* 2001, for example). For this thesis, bicycle exercise MCG and BSPM were recorded in altogether 44 subjects, including 27 patients with single vessel CAD and 17 healthy volunteers.

3.2 Magnetocardiographic exercise measurements

3.2.1 Measurement setup

The exercise MCG measurements were performed at the BioMag Laboratory at Helsinki University Central Hospital (HUCH) in a magnetically shielded room (MSR) (Paavola *et al.* 2000). Fig. 2 illustrates the coil arrangement and positioning of the 67–channel cardiomagnetometer over the chest (Montonen *et al.* 2000). The center of the cardiomagnetometer was placed 15 cm below the jugulum and 5 cm left of the midsternal line. Distance from the chest was set to enable maximal inhale without a contact between the skin and the bottom of the magnetometer.

The laboratory-made non-magnetic ergometer (Takala 1997) used in the measurements is shown in Fig. 3. Fixing the ergometer on the measurement bed takes less than one minute. The bed can be moved freely in and out of the MSR with the ergometer attached. The subject pedals the ergometer in a supine position, feet fastened on the pedals with foot straps which can be opened quickly when necessary. A padded belt around the subject's shoulders (Fig. 3) supports the subject and prevents movement backwards during pedaling.

The ergometer frame and wheel were made of plywood and other materials used in the construction include aluminum, brass and rubber. The bearings of the wheel and pedals were made of polyester. Copper brushes wipe the wheel, leading electric charge to earth and

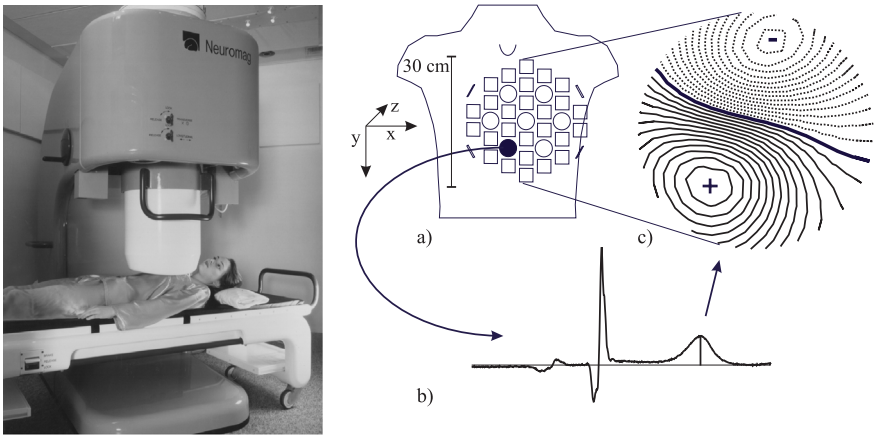

Fig. 2: *A magnetocardiographic (MCG) recording in the BioMag Laboratory. Left: the cardiomagnetometer and the measurement bed. Right: a) Positioning of the MCG sensor array over the chest. The circles show the locations of axial gradiometers detecting $\partial B_z/\partial z$, while the squares refer to planar gradiometer units detecting $\partial B_z/\partial x$ and $\partial B_z/\partial y$. b) An example of signal morphology of one MCG channel, indicated in a). c) An example of an isofield MCG map illustrating the distribution of B_z over the mapped area at the time instant indicated in b). Positive values (solid lines) in the map denote magnetic flux toward the chest.*

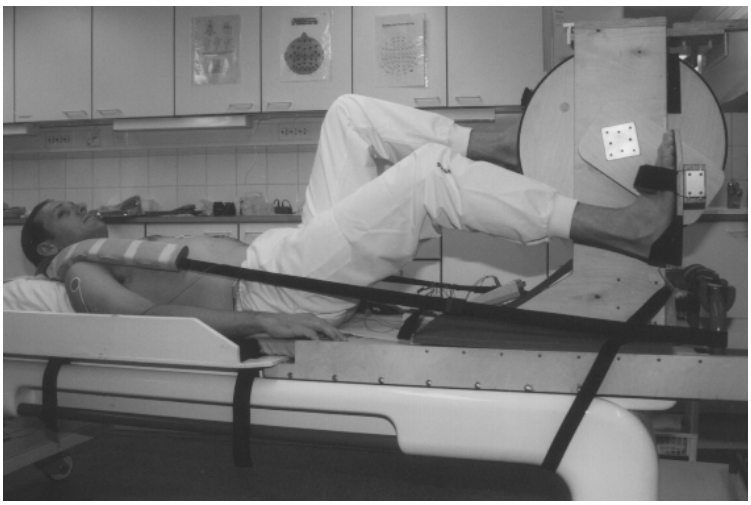

Fig. 3: *The non-magnetic exercise ergometer used in the MCG and the BSPM measurements.*

preventing electric discharge which could damage the sensors of the cardiomagnetometer. A lever (up on the right in Fig. 3) presses a piece of rubber against the wheel providing friction to its rotation. Different load levels can be applied by changing the location and mass of the weights suspended on the lever. Plastic bottles filled with water are used as weights. The ergometer was calibrated to match with a commercially available ECG ergometer (Siemens Ergomed 840L, Germany), also pedaled in supine position.

3.2.2 Measurement protocol

Magnetocardiography A baseline recording of 5 minutes with the subject at rest was made for a reference. In the exercise test, one minute of data were first recorded at rest with the subject's feet attached on pedals. Thereafter, the exercise was started and load on the subject was increased every two minutes. Cessation criteria for the exercise were as recommended by the American Heart Association for the exercise ECG (Fletcher *et al.* 1995). Typical reasons for cessation were severe fatigue or dyspnoea, or chest pain. After exercise, 10 minutes of data were recorded during recovery. The signals were band–pass filtered to 0.03 Hz – 300 Hz, digitised at a sampling frequency of 1 kHz, and stored on a computer hard disk. During the measurements, one physician was inside the MSR while another monitored the recorded signals outside. Audio connection and video monitoring were used for communication between interior and exterior of the MSR during the measurements.

A 12-lead ECG was recorded simultaneously with the MCG using the same data acquisition system and non-magnetic electrodes and connectors. Blood pressure and heart rate were monitored with a Datex–Engstrom AS/3 Compact Monitor, placed outside the MSR.

Body surface potential mapping The same exercise protocol as in the MCG recordings was used in the separate BSPM measurements. Unipolar potentials were recorded with 120 Ag/AgCl electrodes placed on the thorax (Simelius *et al.* 1996, Fig. 4) and three limb potentials with electrodes on the right and left shoulder and the left hip. Average of the limb potentials was used as a reference for the unipolar leads. The thorax electrodes were mounted on 18 strips with an inter-electrode distance of 5 cm. The strips were placed on the subject's thorax vertically and their horizontal spacing was determined using the individual dimensions of the upper body. Forty-five of the electrodes were on the posterior thorax. The front-end electronics of the mapping system was placed inside the MSR. The data were transferred optically to a personal computer controlling the data acquisition outside the MSR. After band-pass filtering from 0.16 Hz to 300 Hz, the signals were digitized with the sampling rate of 1 kHz.

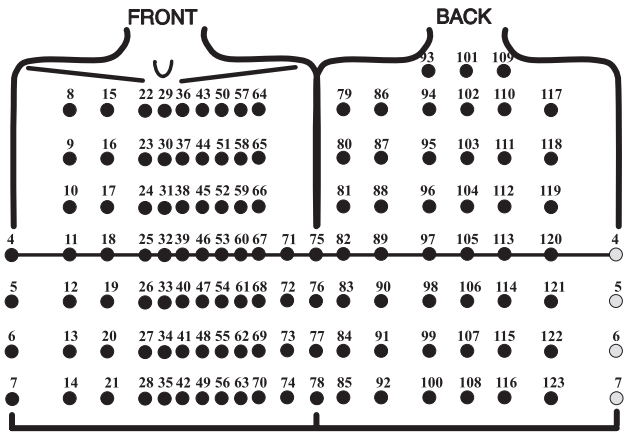

Fig. 4: *The electrode layout of the 123 channel body surface potential mapping system. The vertical line indicates the level of the fourth intercostal space. The three limb leads (channels 1 - 3) are not shown.*

4 Signal processing and analysis

4.1 Signal averaging

Signal averaging is a commonly used method for increasing the signal to noise ratio of the ECG and the MCG recordings. The main objective is to find a representative complex of data with low noise. In most stress MCG studies (Brockmeier *et al.* 1994 and 1997, Hailer *et al.* 1999, and Seese *et al.* 1995, for example) signal averaging has been the first phase of the analysis.

In the exercise MCG and BSPM measurements of this thesis, the low frequency noise caused by heavy breathing was more extensive after exercise than at rest. By signal averaging, effect of baseline drift was reduced, signal baseline was defined and beats with artefacts were excluded. In addition, high frequency noise observed in the signal was reduced. At each time interval of the exercise testing to be analysed, representative complexes of the MCG and the ECG data were obtained by the signal averaging. In Publication I, signals recorded at rest and immediately after cessation of exercise were averaged. In Publications II, III, and VI, also data at 2 and 4 minutes postexercise were evaluated. Due to magnetic noise in some recordings, the MCG data recorded during exercise were not analysed. In Publication VI, only BSPM were recorded and signals just before and immediately after cessation of exercise were averaged.

A software developed in collaboration between the Laboratory of Biomedical Engineering at Helsinki University of Technology (HUT), and the Neuromag Ltd. was employed for signal averaging. The averaging parameters and exclusion criteria for beats with artefacts were adjusted for exercise data. Before averaging, channels with excessive noise in visual inspection were excluded from the analysis. As the first phase of the averaging process, a

template beat with good signal quality in visual observation was selected. The PQ and TP intervals of the template were manually determined on one ECG channel. On each channel, a regression line was fitted on a set of data points at these intervals. In case of high heart rate with a non-detectable TP interval, two consecutive PQ intervals were used. The line was then subtracted from the signals of the template beat on all channels, to establish the baseline level and to reduce low frequency noise.

A range of acceptable data values, called a tube, was formed around the ST segment and the first part of the T wave of the template. The tube was obtained by shifting the template both in time and amplitude coordinates to form envelope curves above and below the template (Paavola *et al.* 1995, Väänänen *et al.* 2000). The shift in time was ±5 ms while the amplitude shift was dependent on the noise level of the signal (see below).

Data on one manually selected ECG channel with high signal amplitude was used in detecting the QRS complexes in each cardiac cycle. The highest signal correlation over the QRS complex was used in determining the time alignment between the template and the first cardiac cycle of data to be processed. On each channel, the baseline-corrected candidate beat was compared with the template and if it did not fit inside the tube, that channel was considered corrupted. Different sensor types (co-axial gradiometers, planar gradiometers, and ECG leads) were evaluated separately and if over 10 % of channels were corrupted in any of the sensor groups, the candidate beat was excluded from the average. Otherwise, the average of the two beats (the template and the candidate) was calculated. The cumulative average was then used in evaluation of acceptance of the next candidate beat. At each interval of the exercise testing to be evaluated, 40 cardiac cycles of data were processed and the result of the signal averaging was the average of the accepted beats. When calculating the tube, the amplitude shift of the template was defined for each sensor type separately and adjusted in such a manner that approximately one half of the beats were included in the average. For example, if less than 20 beats were included, the tubes were broadened and the averaging was repeated.

4.2 Analysed intervals within cardiac cycle

The ischemic injury current alters the bioelectromagnetic signals during the ventricular repolarisation (see section 2). In clinical exercise ECG analysis, the signal amplitude at a time instant of 60 ms or 80 ms after the QRS complex offset (J point) is evaluated (Chaitman 1997). The QT interval duration, however, alters with changing heart rate during exercise testing. Thus, when the observation point is fixed at a given time offset from the QRS complex, different time points in the signal morphology are evaluated. For example, at rest the J point + 80 ms falls in the ST segment whereas in many subjects at peak exercise this time point falls in the up-sloping section of the T wave.

McPherson *et al.* (1985) studied healthy controls with the BSPM during upright exercise testing. They evaluated the potential distributions at different time instants within the cardiac cycle and found that temporally-indexed points on the ST-T waveform during exercise may be misleading. In contrast, the midpoint between the QRS offset and the T wave apex showed little change during exercise in normal subjects. The principle of fixing the observation point at the ST segment to signal morphology was adopted in this thesis. In Publication I, the mid point between QRS offset and the T wave apex was selected for evaluation and in Publications II–VI, the ST segment was defined as the second quarter of the time from the QRS offset to the T wave apex. This allowed time integration of the data and reduced the effect of noise. In addition to the ST segment, the analysis of the MCG and the BSPM data was extended to the T wave. The time from the QRS offset to the T wave apex depends on the spatial location of the ECG lead or the MCG channel evaluated. In Publication I the time instant of T wave apex was determined form the ECG lead II. In Publications II, III, and VI, signals of the seven co-axial gradiometers in the MCG and the precordial ECG leads V_1–V_6 in the BSPM were used. In Publications IV and V, the multichannel MCG data were utilised and the T wave apex was defined as the median over all channels (see section 4.6.3).

4.3 Visualisation of bioelectromagnetic mapping data

MFMs, illustrating the spatial distribution of the magnetic field component normal to the measurement plane, are standard means for illustrating the MCG data at a fixed time instant within the cardiac cycle. For evaluation of a time interval, signals on all channels are integrated over the interval to form an integral map. In this thesis, the integral maps were scaled by the length of the integration time, i.e., they illustrate the spatial distribution of the signal mean over the given interval.

In Publications I–III and VI, group-mean maps of different patient groups were calculated. They present the average signal value over all subjects at each recording location at a given time instant or interval. Difference maps and group-mean difference maps were used for illustrating the change in signal distribution due to exercise. They were formed by subtracting the signal value at rest from the signal value after exercise at each recording location.

A software developed in collaboration between the Laboratory of Biomedical Engineering at HUT, and the Neuromag Ltd. was used for producing the isocontour maps. The method is described in the Appendix of Publication I. Briefly, in both mappings a minimum-norm estimate of a source current distribution was first calculated from the measured data. In the MCG, the source currents were calculated on a slab with the size and form of the measurement plane, 10 cm below it. In the BSPM, sensor surface (= the torso surface) was

scaled to one half of the size, and placed concentrically with the true torso, providing 6–8 cm radial distance from the calculation surface to the electrode surface. The signal values over the triangulated sensor plane in the MCG and over the standard torso model in the BSPM were then calculated from these source current distributions, to obtain the isocontour maps.

4.4 Parametrisation

In stress studies, different physiological conditions augment the spatial and temporal information obtained by the MCG recording. Several parameters have been suggested for detection of ischemia-induced changes in patients, and for describing the essential alterations of the signals recorded in healthy subjects in stress testing. A brief summary of these parameters is presented below.

4.4.1 Signal amplitude

In exercise ECG, detection of CAD is based on the change of the signal amplitude at the ST segment. Also in the first exercise MCG recording, Saarinen *et al.* (1974) determined the ST-shift/R-wave amplitude ratio to quantify the change in the MCG after exercise in a CAD patient. Calculation of the ratio provided a unitless quantity which enabled the comparison between the MCG and the ECG.

In MCG and BSPM recordings made at rest in patients with MI, Lant *et al.* (1990) evaluated the individual map variability V as a root mean square difference between the signal distribution of each subject and mean map of a control group. The parameter was used for quantifying the differences in the amplitude and morphology in a map of each individual, compared to the reference map of the control group. Group mean map variability $\overline{V}$ was used to test the ability of the MCG and the BSPM to distinguish between patients and healthy volunteers at several intervals of the QRST complex. The authors also calculated the group mean normalised variability by dividing $\overline{V}$ by the difference between magnitudes of extrema in the group mean map of the control group.

Brockmeier *et al.* (1994) calculated the range of magnetic field strength (difference of positive and negative signal extrema over the mapped area) at the ST segment at rest and after exercise, to quantify the effect of exercise. Van Leeuwen *et al.* (1999) used the same parameter and evaluated its values over the time-normalised QT interval.

In Publication I, the exercise-induced alteration in the MCG and the BSPM of healthy volunteers was quantified at several time instants of the cardiac cycle by calculating the change in the values of the signal maximum and the minimum over the mapped area. The statistical significance of alteration was used to determine if the extent of response to exercise was different in the MCG, compared to the BSPM. The amplitude ranges of the QRS complex and the ST segment were also evaluated to quantify the exercise-induced alteration in the

MCG and the BSPM.

4.4.2 Magnetic field map orientation

Orientation of an MFM can be used as a rough approximation of the direction of the electric activation of the heart, although it is affected by the inhomogeneities of the body (Tripp 1982). Contrary to the signal amplitude, the orientation is not sensitive to the distance between heart and the MCG sensors (Kandori *et al.* 2001). Given the variability of body size in patients with suspected CAD, this is an important feature. Various methods have been used to measure the orientation of the MFM.

Van Leeuwen *et al.* (1999) defined the MFM orientation as the angle formed by the line joining the centers of gravity of the positive and negative magnetic field values and the right-left line across the torso. They calculated the angle values over the time-normalised cardiac cycle in CAD patients at rest. The angle vs. time traces of healthy controls were used for defining the normal range of angle values and deviations from it were considered abnormal. They also evaluated the width of the magnetic field distribution as the distance between the centers of gravity. In the same study, a two dimensional direction and strength of an equivalent current dipole (ECD) was used to quantify the orientation and strength of the field distribution.

In Publication II, the orientation of MFMs was calculated in two different ways. In the manual analysis, the MFMs of the intervals selected for evaluation were first formed. The signal extrema of each MFM were then connected with a line and the angle between this line and the patient's right-left direction was defined as the MFM orientation. The drawback of this manual method was that both the positive and the negative signal extrema were not always over the mapped area. For example, if only a small proportion of the MFM had a positive signal value, the orientation of the line was hard to define. Likewise, if the magnetic field distribution over the mapped area was totally monopolar its orientation could not be determined.

The other method for quantifying the MFM orientation was based on arrow maps, introduced by Cohen *et al.* (1976b). First, the spatial gradient $(\partial B_z/\partial x, \partial B_z/\partial y)$ of the magnetic field component B_z normal to the measurement plane was calculated over the mapping area. The MFM orientation was then defined as the direction of the largest gradient, and the MFM angle was the angle between this gradient and the patient's right-left line (Fig. 5). The direction of the gradient was defined so that MFM angle values between 0 and 90 degrees were obtained during the T wave in a normal heart.

Recently, Kandori *et al.* (2001) suggested calculation of a total current vector to detect myocardial abnormality. They first calculated current arrow maps, i.e., the spatial derivatives of the component of the magnetic field normal to the measurement plane (Tsukada *et al.* 2000). The total current vector was then obtained as the sum of all current arrows. The

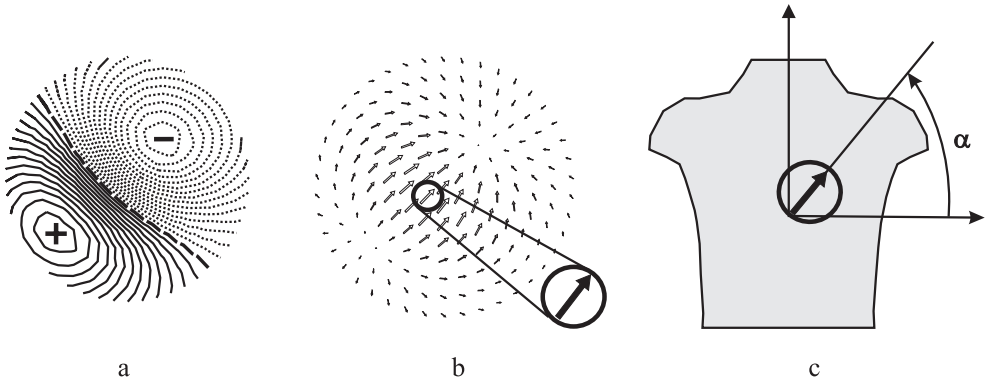

Fig. 5: *Calculation of the orientation of magnetic field maps (MFMs). (a) An example of a MFM. (b) Spatial gradients of the data in (a). The largest gradient and its orientation are indicated with a large arrow. (c) The MFM angle α was measured in respect to subject's right-left line. (From Publication IV)*

orientation of the vector was used as a parameter to separate patients with CAD and patients with hypertrophic cardiomyopathy from healthy controls. The authors calculated the total current vector at two time instants of the ST segment and formed another parameter as the difference of the two vectors.

4.4.3 Correlation between maps

Correlation between two signal distributions provides a measure for the similarity of their spatial form. For example, in stress studies correlation between MFMs recorded at rest and after stress quantifies the exercise-induced alteration. Correlation coefficients calculated for two MFMs and for two BSPMs can be compared directly because they are unitless quantities. Different measurement geometries and mapping areas for the MFM and the BSPM, however, make comparisons between these maps complicated.

Brockmeier *et al.* (1997) calculated the correlation coefficient between MCG maps at rest and after exercise to evaluate the change induced by pharmacologic stress in healthy subjects. Similar analysis was performed with the simultaneously recorded BSPM data. The comparison of correlation coefficients indicated more extensive alteration due to stress in the MCG than in the BSPM during repolarisation. Van Leeuwen *et al.* (1999b) calculated the correlation of MFMs at rest to MFMs during stress in patients with CAD and compared them with correlations in patients without a significant stenosis. In addition, they evaluated the change in spatial form of the QRST integral maps by calculation of Karhunen-Loeve transform. The non-dipolar content of the maps was evaluated by subtracting first three eigenvectors from a map generated by 12 first eigenvectors.

In Publication I, correlation coefficient between the MFMs and between the BSPMs was calculated for signal distributions recorded at rest and the corresponding distributions at

cessation of exercise. The calculation was performed in each subject separately and the mean correlations in the MCG and the BSPM were compared. Group mean maps showing the average distributions at rest and after exercise were also formed and their correlation was evaluated.

4.4.4 QT interval dispersion

Spatial dispersion of the QT interval duration (from the QRS complex onset to the T wave offset) describes the heterogeneity of ventricular repolarisation on the basis of the temporal range of the QT intervals. The distribution of the QT interval duration has been used as an index for identifying patients with CAD by the MCG both at rest (Van Leeuwen *et al.* 1999) and in stress studies (Hailer *et al.* 1999, Van Leeuwen *et al.* 1999b). In these studies, the QT interval duration was determined on all channels and the QT time dispersion was evaluated over the mapped area. The spatial distribution of the QT duration was also evaluated using a Smoothness Index (SI) which quantifies the differences of the QT time values in the neighborhood of the individual channels. The value of the SI increases with greater spatial heterogeneity of the repolarisation process. The intra-individual effect of stress was assessed by the change in the QT interval duration on all channels.

4.4.5 Source current distributions

Several source model parameters have been used to analyse the measured field distribution in stress MCG studies. Seese *et al.* (1995) calculated a two dimensional current density estimate (CDE) to visualise and localise exercise-induced injury current by the MCG. Brockmeier *et al.* (1997) used components of electric and magnetic dipole to obtain first-order approximations of the flow and vortex part of the source current during stress in healthy subjects. Pesola *et al.* (1999) calculated the CDE on the left ventricular epicardium to localise exercise-induced ischemia.

4.5 Finding the optimal recording locations

In the 12-lead ECG, where spatial information is limited, the ischemia parameters are determined from signals on each channel separately. The performance of such parameters is dependent on the recording location. When a spatially extensive mapping is available it can be utilised in finding the optimal recording locations over the thorax.

Discriminant index (DI), suggested by Kornreich *et al.* (1991), was used in Publications III and VI to study the optimal sensor locations for ischemia detection by the BSPM and the MCG. For each sensor location, DIs were evaluated for parameters detecting ischemia-induced changes in signal amplitude at the ST segment and the T wave. To calculate the DI at a given sensor location, average value of a parameter in the control group was first

subtracted from the average of the patient group. The difference was then divided by the corresponding standard deviation (SD) over all subjects to get the DI. Thereby, the DI quantifies the mean difference in the parameter value between patients and controls, divided by the inter-individual variation of the parameter. A large difference between patients and controls in the average value of a parameter does not indicate good performance in separating the groups if inter-individual variation is extensive. The positive DI values indicate ischemia-induced increase in the parameter and a negative DIs indicate its decrease due to ischemia. Sensor locations with the highest absolute values of DI were considered as the best ones for ischemia detection by the parameter under study.

4.6 Beat-to-beat analysis

A method for beat-to-beat analysis of multichannel exercise MCG data was developed in Publication IV. The aim was to extract and utilise information on the recovery dynamics, and to avoid some of the drawbacks encountered in the analysis of the signal averaged MCG data. In signal averaging, the analysis was focused on few stages of the exercise testing only, and the continuous development of the MFMs could not be monitored. The alignment of the complexes in the averaging was made on the basis of the QRS complex which may hamper the analysis of the ST-T segment. In the beat-to-beat analysis, better focusing on the repolarisation period of the cardiac cycle was obtained. In addition, the baseline estimation was improved by a non-linear method implemented for the beat-to-beat analysis.

4.6.1 QRS complex detection

One ECG channel with high QRS complex amplitude was used for determining the trigger points within each QRS complex. First, the time instant of the steepest slope was found in one template beat. The highest correlation with the template was then used to define the corresponding time instant in all cardiac cycles.

4.6.2 Baseline estimation

Signal mean over an interval of 20 ms at the PQ segment was defined as the signal baseline. A constant offset from the trigger time to the beginning of the baseline interval was first determined in a template complex. The same offset was then used in all beats to define the baseline nodes through which the baseline estimate was calculated. A method developed by Meyer and Kaiser (1977) was used for calculating the non-linear baseline estimate for signals on each channel. The estimate was subtracted from the signals to reduce the low frequency baseline drift. In the template, also time-offsets from the trigger time to QRS complex onset and QRS complex offset were determined and they were used in determining the corresponding time instants in all beats.

The baseline estimator uses only data at the PR intervals. Since the low-frequency heart activity is not admitted into the baseline estimate, it can not be subtracted from the data. Thereby, in principle, the ST segment and T wave will not be distorted. The performance of the baseline estimator is, however, strongly dependent on the ratio of heart rate and frequency of the baseline noise. As the heart rate determines the sampling frequency of the baseline, the higher the heart rate, the better estimator is obtained. Meyer and Kaiser (1977) demonstrated empirically that when the baseline sampling rate is four times higher than that of a baseline noise component of the signal, more than 88 % of that noise component is removed.

4.6.3 Determination of the T wave apex

The time instant of T wave apex is not the same in every recording location. Bi-phasic T waves may also hamper the detection of the T wave on some channels. In Publications IV and V, data on all channels were utilised in determining one T wave apex time to be used in processing of the data on each channel. A rough estimate was first found for the T wave offset. Here, the simple formula originally introduced by Fridericia (1920) was used to determine the *T offset* (in ms):

$$T\ offset = QRS\ onset + 450 \times (RR\ interval)^{1/3}, \tag{3}$$

where *RR interval*, is the duration of the time interval between two consecutive R deflections in ms.

On each channel, the T apex was defined as the highest signal deviation from the baseline at the ST-T interval. The time instant of T apex for the whole mapping was then defined as the median of T apex times over all channels. In this manner the bi-phasic T waves, typically found on channels close to the spatial region of zero amplitude T waves, had only a small effect on the time selection. The method is also less sensitive to artefacts and noise than, for example, the determination of the time instant of the highest T wave amplitude over all channels, or the instant of T wave apex on a single channel. In visual evaluation, the T apex times determined in this way coincided well with the T apexes of the highest T waves over the mapped area.

4.6.4 Extraction and filtering of the magnetic field maps

The ST segment was defined as the second quarter of the time interval from the QRS offset to the T apex. MFMs were extracted from each complex by calculating the signal mean on each channel over the ST segment and over the T apex ± 10 ms. To increase the signal to noise ratio of the MFMs both at the ST segment and the T wave, they were mean filtered with a window length of 11 MFMs. This was done by replacing each MFM by the mean

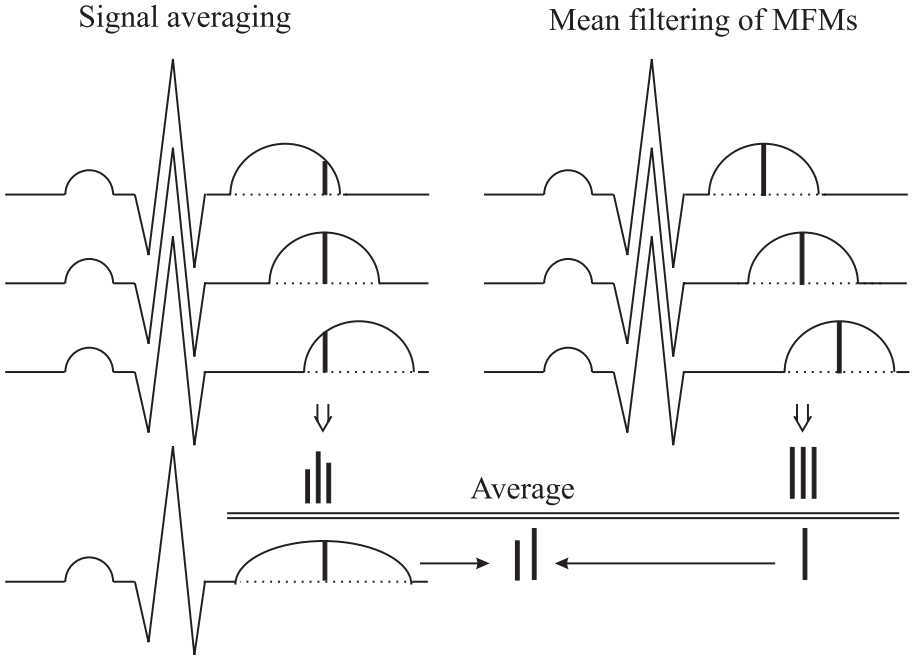

Fig. 6: *Schematic illustration on the difference between signal averaging (left) and mean filtering of magnetic field maps (MFMs, right). The complexes on the top of the figure illustrate data of consecutive cardiac cycles with increasing QT interval duration on one channel. Vertical bars indicate the data which affect the amplitude of the T wave apex in the result of the processing. On the bottom of the figure, the result of the processing is illustrated. Signal averaging results in an averaged complex and mean filtering results in the mean amplitude of the T wave. The vertical bars illustrate the T wave amplitude, obtained by both methods. In signal averaging, the changing QT time causes a damped and prolonged T wave. The result of the MFM filtering is the average of the T wave apex amplitudes over all complexes, as desired.*

of 11 maps, extracted from consecutive beats of data. Here, the map under processing, 5 MFMs from cardiac cycles preceding it, and 5 MFMs from beats following it were used.

Mean filtering of maps vs. signal averaging.

Duration of the QT interval is affected for example by breathing and heart rate. In signal averaging, if complexes to be averaged are aligned according to the QRS complex, the T wave apex in one complex does not coincide with the T wave apexes of the other complexes with different QT times. Fig. 6 shows a schematic illustration on the differences between conventional signal averaging and mean filtering of MFMs, used in the beat-to-beat analysis in Publications IV and V. In the figure, data of three consecutive cardiac cycles with increasing QT time are presented. Vertical bars indicate the data affecting the amplitude of the T wave apex obtained as the result of processing. Due to changing QT duration, the T wave in the averaged data (left side of the figure) is longer than in the individual beats. It

also has a lower peak amplitude since data from both up-sloping and down-sloping section of the T wave are included in the average. In the beat-to-beat analysis, the data at T wave apex are first extracted from each complex. Thereafter, the mean of these data is calculated and the result is independent of the QT duration. The ST segment in the signal averaged data is blurred through a similar process as that described above for the T wave.

As the MFMs are extracted from individual cardiac cycles, the temporal signal properties within the beat are lost in the MFM averaging. Therefore, it can not be used for example for analysis of QT duration. Also, contrary to selective signal averaging, selective MFM averaging was not performed in this thesis. Instead, MFMs from all cardiac cycles were used in the analysis, independent of signal quality.

4.7 Heart rate adjustment of ischemia-induced change

4.7.1 Electrocardiography

ST segment depression in the ECG depends not only on the extent of underlying coronary artery stenosis, but also on the metabolic activity of the heart. That is, the severity of ischemia increases with ongoing cardiac work during exercise testing. Basic principle in heart rate (HR) adjustment is to relate the ST segment depression to this additional factor. Myocardial oxygen consumption is directly related to higher HR during exercise (Okin and Kligfield, 1995). From a physiological point of view, HR adjustment of ST depression normalises the increasing magnitude of apparent ischemia during exercise (as measured by changes in the ST segment) for the corresponding increase in myocardial workload (as measured by changes in HR) that leads to ischemia in the presence of coronary disease.

Two methods of HR adjustment of ST segment depression have evolved in the 12-lead ECG (Kligfield 1989, Okin and Kligfield 1995). The simpler ST-segment/HR index is derived by dividing the maximal change in ST depression during exercise by the change in HR from rest to peak exercise. In the other method, ST-segment/HR slope calculation, linear regression analysis is performed from the end of exercise to data at earlier stage during exercise in each lead. The highest ST-segment/HR slope with a statistically significant correlation coefficient among all leads, including bipolar ECG lead CM_5 but excluding aVR, aVL, and V_1, is taken as the test finding.

4.7.2 Magnetocardiography

The data at the end of each stage of exercise are used in the calculation of the ST-segment/HR index and the ST-segment/HR slope in the ECG (Kligfield 1989, Okin and Kligfield 1995). In contrast, in Publications IV and V the MCG beat-to-beat analysis focused on the data recorded during the recovery, due to excessive magnetic noise during exercise in some of the recordings. Also, each cardiac cycle recorded postexercise yielded one data point for the

regression analysis.

The orientations of the MFMs at the ST segment during the recovery period, and the orientations of the MFMs at the T wave apex from one to ten minutes postexercise were the source data for quantifying the HR adjusted change in the MCG. The mean and the SD of the angle values were first calculated in each subject. To reject artefacts, angles deviating more than 2×SD from the mean were discarded from further analysis. Thereafter, the values of MFM angles were plotted against the corresponding instantaneous HR values, calculated from the RR interval duration, and a regression line was fitted to the data. The absolute value of the line slope was calculated both for the ST segment data (MFM ST/HR slope) and the T wave data (MFM T/HR slope) of each subject.

The HR adjustment method, applied to the MFM rotation in Publications IV and V, resembles the previously reported ST-segment/HR slope calculation in the ECG as it incorporates in the regression analysis all data points during the recovery. It does not, however, focus on the most rapid change in the MFM orientation and in that respect it is similar to the ST-segment/HR index.

5 Studies on healthy subjects and patients with CAD

The objectives and main results of the studies on healthy controls and CAD patients, reported in Publications I–III, V, and VI, are summarised in this chapter. The results are discussed in section 6.

5.1 Magnetic and electric mapping in healthy subjects

The aims of the study presented in Publication I were twofold; 1) to clarify the normal response to exercise in the MCG and 2) to study the possible differences between the MCG and the BSPM. Knowledge of the exercise-induced alterations in the MCG of healthy subjects is essential when clinical applications of exercise MCG are developed. On the other hand, since the first recording of the MCG by Baule and McFee (1963), there has been discussion on whether the MCG contains information complementary to the ECG. The changes found in the MCG of healthy subjects, but not in the simultaneous ECG, during physical and pharmacological stress (Brockmeier *et al.* 1994 and 1997) motivated a further study on exercise MCG in healthy volunteers.

The study group in Publication I was formed by 12 middle-aged healthy volunteers (1 female) with normal exercise ECG, echocardiogram and no history of cardiovascular disease. The exercise MCG and BSPM were recorded as described in section 3.2. The signal averaged data (see section 4.1) at rest and immediately after exercise were analysed.

5.1.1 Signal range

Signal range of the QRS complex (from the onset to the offset of the QRS complex) and the ST segment (from QRS offset to the midpoint between QRS offset and T apex) was measured as the difference of the highest and the lowest signal value over the mapped area during the corresponding interval. The QRS complex signal range was found to diminish and the ST segment range to increase in the MCG, due to exercise. In the BSPM, however, no significant alteration was observed.

5.1.2 Amplitudes of signal extrema

In the MCG, an amplification of the signal minimum over the mapped area took place both at the ST segment and at the T wave apex as a response to exercise. At the ST segment, the amplification was found both at an instant fixed in time (60 ms after QRS offset; J_{60}) and at an instant fixed in signal morphology (midpoint between QRS offset and T wave apex). At J_{60}, also the value of signal maximum amplified in the MCG and at the T wave the signal maximum became smaller as a response to exercise. Contrary to the MCG, no significant change was found in any of these parameters in the BSPM.

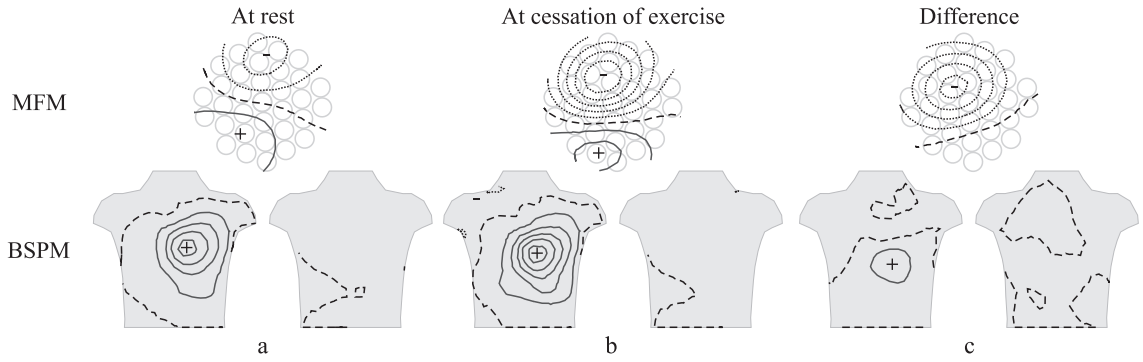

Fig. 7: *Group-mean isocontour maps of the healthy volunteers at J_{60}: MFM (above) and BSPM (below) a) at rest and b) after exercise. c) the difference maps. The step between two consecutive isocontours is 0.5 pT in the MFMs, and 50 μV in the BSPMs. Solid lines indicate positive and dotted lines negative field or potential. Broken curve indicates the zero signal. In the MFMs, positive values indicate magnetic flux toward the chest. In the potential maps, torso silhouettes represent the potential over the anterior chest (left), and over the back (right). (From Publication I)*

5.1.3 Spatial patterns

The spatial distribution of the MCG and ECG signals was evaluated qualitatively using group-mean maps at rest and at cessation of exercise (see section 4.3). Difference maps were formed for illustrating the exercise-induced change in the signal distribution (Fig. 7).

QRS complex. The difference map in the MCG indicated a decrease in the QRS integral value due to exercise over most of the mapped area. In the BSPM, the change due to exercise in the spatial pattern of the QRS complex integral maps was small. However, the integral value decreased and the group-mean difference map had a negative area over the precordium.

ST segment. Fig. 7 illustrates the group-mean MFMs and BSPMs of the ST segment at J_{60} at rest and at cessation of exercise. The difference maps indicate a decrease in the MCG signal value due to stress but in the BSPM only a relatively small change is observed. In qualitative evaluation, the group-mean maps at the mid point between the QRS offset and the T wave apex were found similar to maps at J_{60}.

T wave. The group-mean and difference maps of the MCG and the BSPM at the T wave apex are shown in Fig. 8. In the MCG, exercise resulted in a shift of the zero field line downward and to the patient's right. In accordance with the ST segment, the difference map (Fig. 8) indicated a decrease in the signal value at the T wave apex. In the BSPM, the difference map showed some alteration in signal values due to stress but the amplitude change was not significant.

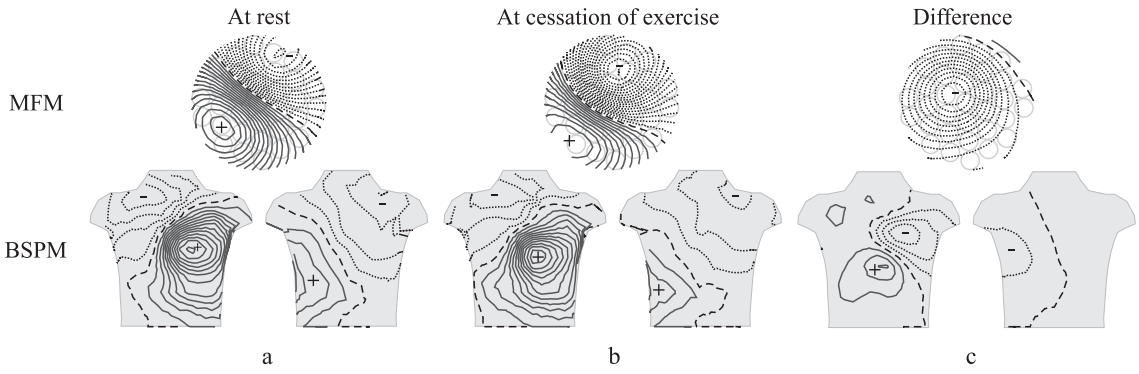

Fig. 8: *Group-mean isocontour maps at the T wave apex: MFM (above) and BSPM (below) a) at rest and b) at the cessation of exercise. c) the difference maps. In the MFMs the step between two consecutive isocontour lines is 0.5 pT, and in the BSPMs it is 50 μV. The format is the same as in Figure 7. (From Publication I)*

5.1.4 Correlation of maps at rest with maps at exercise

The correlation of maps at rest with those recorded postexercise was calculated in all individuals. The correlation was, on the average, higher in the BSPM than in the MCG at the ST segment and the T wave but the difference was not significant.

5.1.5 Variation between the subjects

In Publication I, the variation of the MCG and BSPM signal distributions within the study group was evaluated by calculating the mean correlation between each individual map and the group-mean map. The usefulness of a group-mean map and a group-mean difference map depends to a great extent on the variation of the individual maps within the study group. In case of high variation, they do not provide an optimal charcterisation of the features of the maps in the study group. The inter-individual variation is of interest also when evaluating the value of the results as reference data for future studies.

In general, the variation in the maps was more extensive in the MCG than in the BSPM. In both mappings the highest correlation was found at the T wave, which had a higher signal amplitude and better signal to noise ratio than the ST segment. The highest variation between different subjects was found in the QRS complex integral maps which are to a great extent affected by the signal morphology, since both negative and positive deflections contribute to the integral value.

5.2 Magnetic field maps in patients with coronary artery disease

Detection of exercise-induced ischemia in patients with single vessel CAD was studied in Publication II. The aim was to find features of the MCG signal, altered by ischemia, and to develop a parameter which could be used in ischemia detection. Forty-four subjects were

studied with exercise MCG and simultaneous 12-lead ECG. The patient population consisted of 27 CAD patients with a significant (>50 % luminal diameter) stenosis in one of the major coronary branches. Twelve patients had a stenosis in the left anterior descending (LAD), seven in the left circumflex (LCX), and eight in the right coronary artery (RCA). In addition, a control group of 17 healthy volunteers was studied.

The measurement equipment and protocol used in the recordings are described in section 3.2. The signals recorded at rest, immediately after exercise as well as 4 minutes postexercise were averaged as described in section 4.1. From each averaged complex, MFMs were formed using data at the ST segment (signal mean over the second quarter of the time interval from the QRS offset to the T wave apex) and at the T wave apex. Orientations of the MFMs were measured both manually and by using the gradient method, as described in section 4.4.2. Both methods yielded approximately similar results and in the following those obtained with the gradient method are presented. Group-mean MFMs were calculated to describe the signal distributions in the study groups.

5.2.1 Orientation

The principal finding in Publication II was that exercise-induced ischemia caused a rotation of the MFMs at the ST segment and at the T wave apex. Orientations of the MFMs at these time instants were compared in patients and controls.

Rest. Because of low signal amplitude, noise hampered determination of MFM orientation at the ST segment at rest. Variation between subjects in the MFMs at the ST segment was extensive and a wide distribution of angle values was obtained even within the control group. Only the subgroup of patients with stenosis in RCA had a significantly different MFM orientation compared to the control group. Other patient subgroups and the pooled CAD group did not differ from controls in respect of the MFM angle at the ST segment. At the T wave apex, the MFM orientations were more consistent. Still, none of the patient groups differed significantly from the control group in respect of the MFM orientation.

Immediately after exercise. At cessation of exercise, the MFM orientation at the ST segment was different in the pooled CAD patient group and in the subgroups of patients with stenosis in LAD or RCA, when compared to the control group. Fig. 9 shows the ST segment group-mean maps of the controls and CAD patients at rest and at the cessation of exercise. The arrows illustrate the manual and the gradient-based measurement of the MFM orientation. The group-mean map of the CAD patients is rotated after exercise compared to rest, while in the controls the rotation is smaller. The MFM orientation at the T wave apex was not significantly different in any of the patient groups compared to the control group.

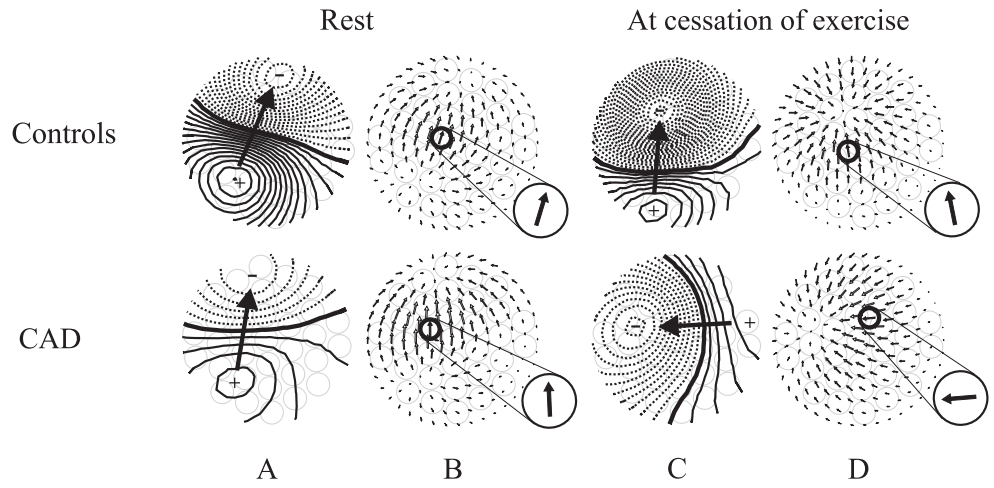

Fig. 9: *Group-mean MFMs of the ST segment (A, C) and the corresponding spatial field gradients (B, D) of healthy controls and coronary artery disease patients (CAD) at rest and at cessation of exercise. In A and C, the step between two consecutive isofield lines is 0.1 pT and the arrow indicates the manually determined map orientation. In B and D, the maximum spatial gradient is indicated by the circled arrow. (From Publication II)*

Four minutes after exercise. In contrast to what was observed at the cessation of exercise, the orientation of the T wave MFM at 4 minutes postexercise was different in the CAD patient group than in the control group. Also the in the subgroup of patients with stenosis in RCA, the MFM orientation at the T wave differed from the orientation of the control group. At the ST segment, the MFMs angles in the pooled CAD patient group and in subgroups of patients with stenosis in LAD or LCX were higher compared to the control group.

5.2.2 Rotation

Rotation of the T wave apex MFM from rest to 4 minutes postexercise was more extensive in the pooled CAD patient group than in the control group. This was the case also with the subgroup of patients with stenosis in RCA. That subgroup had also a more extensive MFM rotation compared to the subgroups of patients with a stenosis in LAD or LCX. Compared to controls, the MFM rotation at the T wave apex from rest to cessation of exercise was more extensive only in the subgroup of patients with stenosis in RCA. Rotation of the MFM at the ST segment was not evaluated due to low signal amplitude at rest.

5.2.3 Amplitude

At rest the ST segment MFMs had a low amplitude, i.e., the values of signal extrema were often below 0.1 pT. Exercise amplified the values of signal extrema over the mapped area at the ST segment both in the patients and in the controls. Thereby, the maximum ST

segment depression over the mapped area did not differ between patients and controls.

5.3 Magnetic and electric mapping in patients with coronary artery disease

Publication III aimed at identifying the optimal recording locations in the MCG and the BSPM for detection of exercise-induced ischemia. The study population was the same as in Publication II, except for three patients (one in each subgroup of different stenosed vessel) whose BSPM data were corrupted. Signals recorded at rest, immediately after exercise, and 4 minutes after exercise were averaged. The MCG and BSPM data of the ST segment (signal mean over the second quarter of the time interval from the QRS offset to the T wave apex) and of the T wave apex were extracted from each averaged complex.

To identify the optimal recording locations for detecting ischemia-induced alteration in the amplitude of the ST segment and the T wave, DI maps were calculated for both the ST segment and the T wave data in the MCG and the BSPM (see section 4.5). The extrema of the DI maps were selected as the optimal recording locations for detecting ischemia-induced increase (positive extremum) or decrease (negative extremum) in the parameter evaluated.

The ST segment group-mean maps of the CAD patients and controls at rest and at cessation of exercise are shown in Fig. 10. The corresponding DI maps are illustrated in Fig. 11. In the left panel of Fig. 11, negative DI extremum suggested that the optimal recording location for separating CAD patients from controls by ST segment depression in the ECG was at the lower left side, below the lead V_5. The distribution of positive DI values shows that, compared to controls, the ST segment in the CAD patients was elevated over

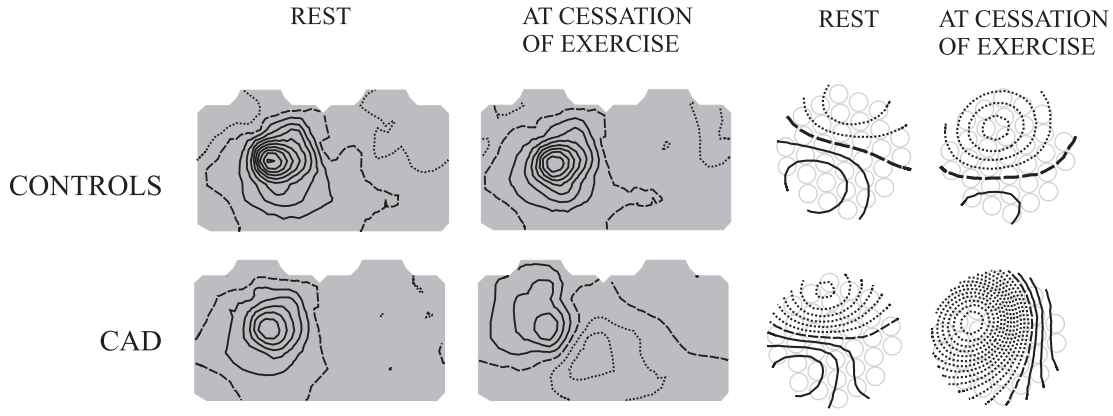

Fig. 10: *Group-mean BSPMs (left) and MFMs (right) of the ST segment at rest and at cessation of exercise. Top: healthy controls; bottom: CAD patients. The step between two isocontour lines is 0.025 mV in the BSPM and 0.1 pT in the MCG. Solid lines denote positive signal values and dotted lines indicate negative values. Zero signal is indicated by a dashed line. (From Publication III)*

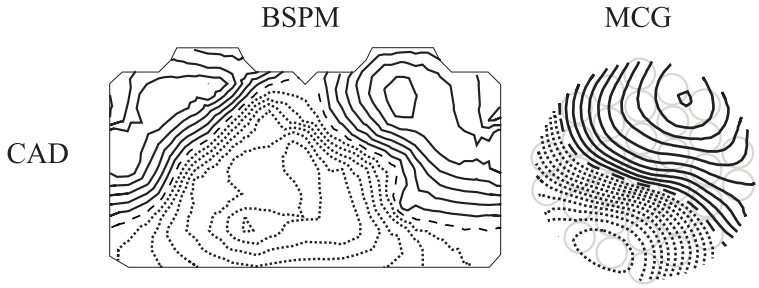

Fig. 11: *DI maps of the pooled CAD patient group at the ST segment at cessation of exercise. The step between two isocontour lines is 0.2 in the BSPM and 0.1 in the MCG. Positive values are denoted by a solid line and dotted lines indicate negative values. (Modified from Publication III)*

the upper right anterior and right posterior thorax at cessation of exercise. The analysis suggested that this area is optimal for detecting ischemia by the ST segment elevation.

The right panel of Fig. 11 shows the CAD patient group's DI map of the ST segment in the MCG at cessation of exercise. The extrema of the DI map suggested that optimal sites for ischemia detection by ST elevation and ST segment depression located over the upper left part of the thorax and over the central inferior part of the chest, respectively. The locations of the highest and lowest index values for pooled CAD patient group and for patient subgroups are indicated in Fig. 12 for the MCG and in Fig. 13 for the BSPM. The

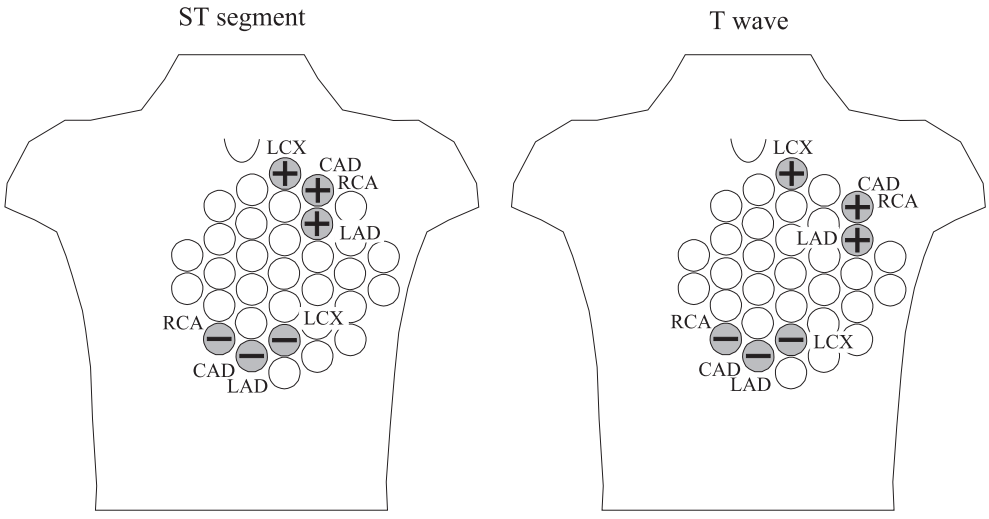

Fig. 12: *Recording locations in the MCG with the highest and the lowest DI value in all patient subgroups with a different stenosed vessel, and in the pooled CAD patient group. Left: ST segment at cessation of exercise. Right: T wave apex 4 minutes postexercise. The plus (+) character indicates that the highest DI value of the specified patient group was found on that location. Abbreviation next to the sign denotes the patient group. Correspondingly, the minus (−) character indicates the most negative DI value.*

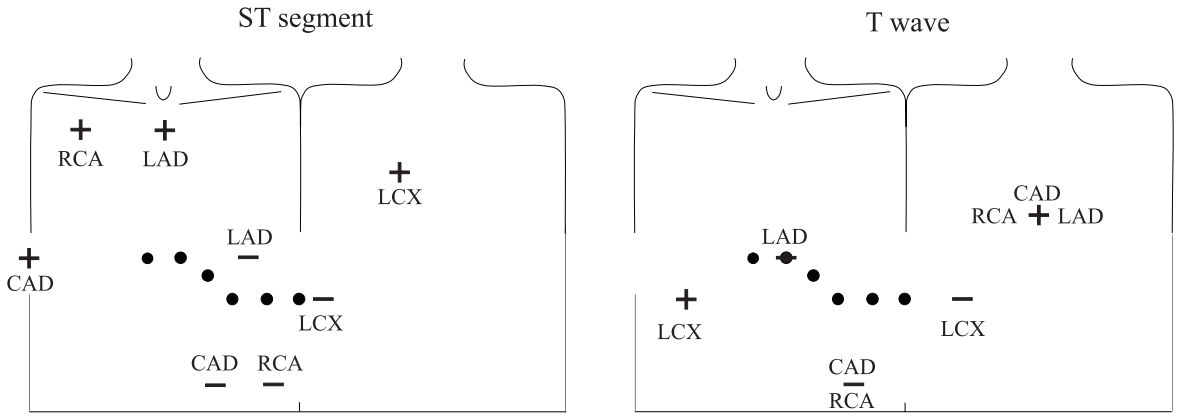

Fig. 13: *Recording locations in the BSPM with the highest and the lowest DI value in all patient subgroups with a different stenosed vessel, and in the pooled CAD patient group. Left: ST segment at cessation of exercise. Right: T wave apex 4 minutes postexercise. The plus (+) character indicates that the highest DI value of the specified patient group was found on that location. Abbreviation next to the sign denotes the patient group. Correspondingly, the minus (−) character indicates the most negative DI value. The recording locations of the ECG leads V_1–V_6 are indicated with black dots.*

results are presented for the ST segment immediately after exercise and for the T wave 4 minutes postexercise.

By comparing the CAD patients' group-mean MCG maps (Fig. 10) and the DI map in Fig. 11 it can be noted that the optimal recording location for detecting ST segment depression deviated from the location of the maximum depression in the group-mean map. In addition to the ischemia-induced changes in the patients, the value of DI was affected by the exercise-induced change in controls and the inter-individual variance over the study population (see section 4.5).

After finding the optimal recording locations, their performance was tested by evaluating the statistical significance of difference in signal amplitude between patients and controls. At the optimal MCG and BSPM recording sites, all parameters (ST segment depression and elevation, T wave amplitude increase and decrease) were different in the CAD patient group than in the control group. For details concerning the results of the patient subgroups see Publication III.

5.4 Heart rate adjustment in exercise magnetocardiography

In Publication V, the beat-to-beat analysis method developed in Publication IV (section 4.6) was applied in a study population of 17 healthy controls and 24 patiets with single vessel disease. The aim was to evaluate the performance of HR adjusted change in MFM orientation in detection of exercise-induced ischemia. The results were compared with the results of unadjusted MFM orientation as well as with the results obtained by the 12-lead ECG both with

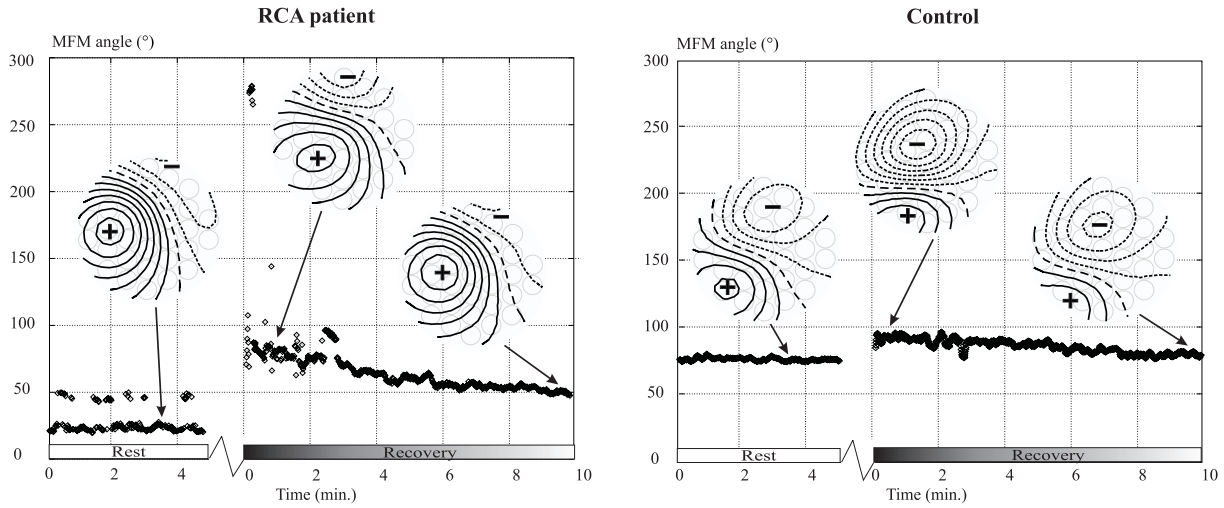

Fig. 14: *ST segment MFM angle of each cardiac cycle recorded in one patient with stenosis in RCA (left) and in one healthy control (right), and examples of field distributions. The MFM angles at rest and during the recovery from exercise are plotted against time. Data during exercise has been omitted. After exercise the angle is tilted compared to rest, and during the recovery it returns close to the baseline value. In the patient, the rotation due to exercise is more extensive than in the control. Arrows indicate the time instants and angle values for the MFMs. The step between two isofield lines in the maps is 0.5 pT. (Modified from Publication V)*

and without HR adjustment. The development of the MFMs and their orientation during the recovery period of exercise testing was also studied. The MCG analysis was performed as explained in section 4.6 and the change in MFM orientation was adjusted to HR, as described in section 4.7.2.

The HR adjusted MFM rotation was more extensive in the CAD patient group than in the control group during the recovery period of exercise testing. At the ST segment, the regression lines of the MFM rotation had higher slope values in the pooled CAD patient group, as well as in all patient subgroups than in the control group. Likewise, the regression line slopes at the T wave were steeper in all CAD patient groups than in the control group. An example of the development of the ST segment MFM orientation in a patient with an RCA stenosis and in a healthy control is given in Fig. 14. In Fig. 15 the data of the same subjects is plotted against the HR, and the regression lines illustrate the HR adjustment of the change in the MFM angle.

In some CAD patients the MFMs had a monopolar pattern without a clear maximum of the spatial MCG signal gradient, and changes in its location were found during recovery. Because the maximum gradient was used to determine the MFM orientation, sudden changes in its location resulted in abrupt changes in the MFM angle and gave rise to especially high regression line slope values in such patients. This resulted in a high standard deviation in the

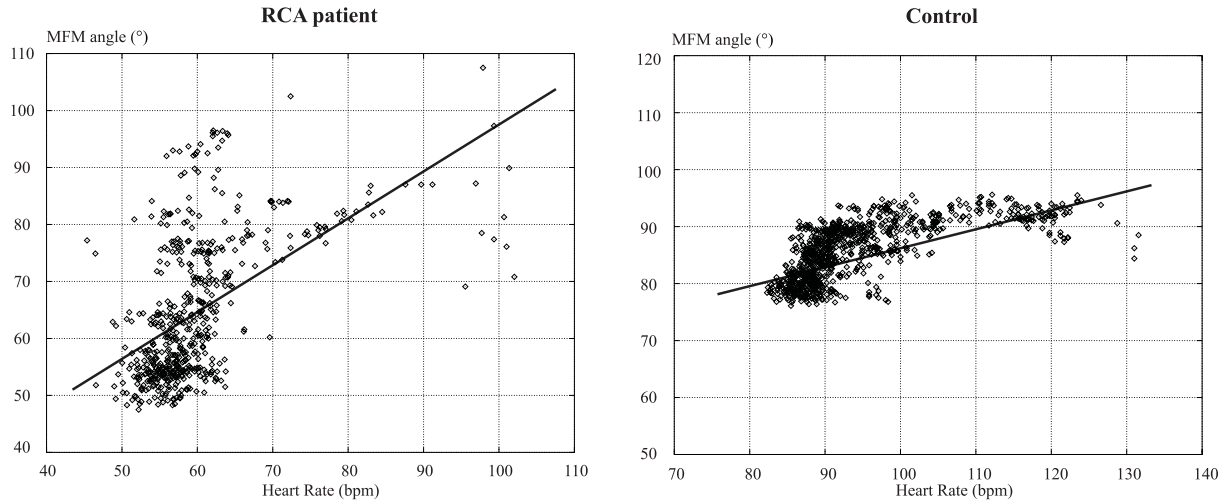

Fig. 15: *The MFM angle data of Fig. 14, plotted against the HR. Data values considered outliers have been excluded, as explained in section 4.7.2. Lines through the data indicate the regression lines used for the quantification of the change in the MFM angles. For the patient the line slope is 0.81 °/bpm (beats per minute) and for the control it is 0.34 °/bpm. (Modified from Publication V)*

patients' MFM angle parameters. In the control group, however, the average slope values and their standard deviations were small. The variation between the subjects in the dependence between MFM orientation and HR was extensive during the 10 minutes of recovery. In general, it was not linear in the patients. The linear regression analysis was used merely to quantify the change of the MFM orientation and to adjust it with the corresponding change of the HR.

5.4.1 Receiver operator characteristic curves

Fig. 16 shows the receiver operator characteristic (ROC) curves of the parameters evaluated in Publication V. The HR adjusted MFM rotation at the ST segment had a higher sensitivity to CAD than the MFM orientation at the ST segment immediately after exercise at almost all values of specificity. It also had a higher or equal sensitivity compared to the HR adjusted ST segment depression in the 12-lead ECG at all values of specificity. At the T wave, the HR adjusted MFM rotation had an equal or higher sensitivity than the MFM orientation at the T wave 4 minutes postexercise, independent of the required specificity. The areas under the ROC curves (AUCs) of all these parameters are indicated in Fig. 16.

5.5 Ischemia detection by body surface potential mapping

Seventy subjects were studied with BSPM during exercise in Publication VI. The study population consisted of 18 patients with triple vessel CAD and a history of one or more MIs,

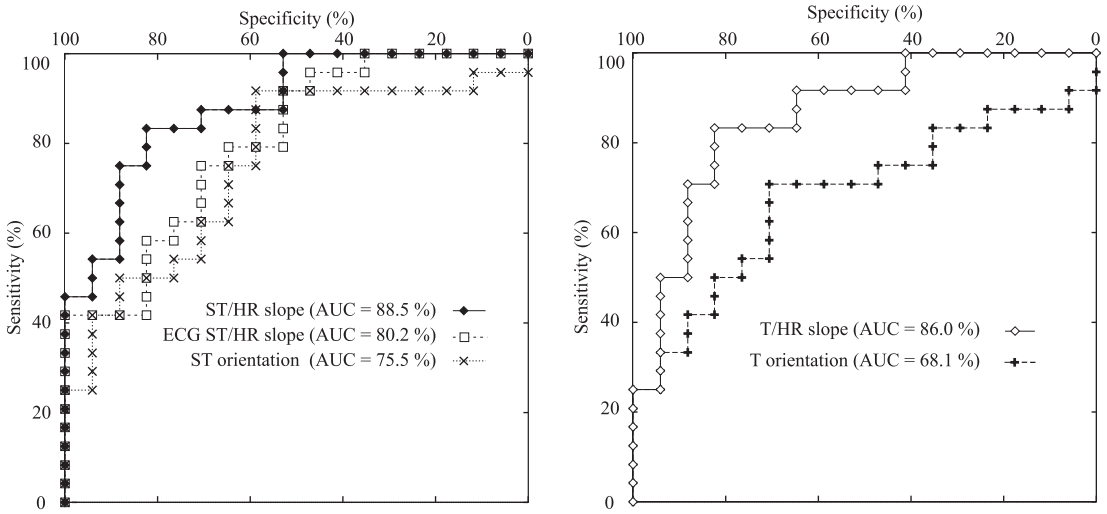

Fig. 16: *Left: ROC curves for HR adjusted MFM rotation at the ST segment (ST/HR slope), HR adjusted ST segment depression in the ECG (ECG ST/HR slope), and MFM orientation at the ST segment in signal averaged data immediately after exercise (ST orientation). Areas under ROC curve (AUCs) are indicated as percentages. Right: ROC curves and AUCs for the HR adjusted MFM rotation at the T-wave (T/HR slope) and for the MFM orientation at the T-wave 4 minutes postexercise (T orientation). (From Publication V)*

27 patients with single vessel CAD, and 25 healthy controls. The aims were to evaluate the performance of ST segment slope ($\mu V/s$) as an independent indicator of exercise-induced ischemia and to find its optimal recording locations. In addition, the optimal locations for ischemia-induced ST segment depression were studied.

The patients with triple vessel CAD were classified into three subgroups according to the main ischemia region (LAD, LCX, RCA). The classification was based on findings in thallium perfusion single photon emission computed tomography stress imaging with redistribution imaging at 4 hours, and on coronary angiography. The subgroups with anterior (LAD), posterior (LCX), and inferior (RCA) ischemia were appended with the patients with the corresponding single vessel disease.

Signals at rest, during the final exercise period, and immediately after cessation of exercise were averaged. The data recorded immediately after exercise performed better in ischemia detection than the data during exercise. Therefore, the results are presented for these data. The ST segment amplitude at 60 ms after the J-point (J_{60}) and the ST segment slope ($\mu V/s$) from J-point to J_{60} were calculated in each lead. The slope was determined by fitting a regression line on the data at the ST segment. DI was used for finding the optimal locations for detecting ischemia-induced alteration in the ST segment level and slope.

Fig. 17 shows the group-mean maps of the ST segment level and slope immediately after exercise in healthy controls and in the subgroups of patients with different ischemic regions. Compared to the controls, the patients with CAD showed ST segment depression and more

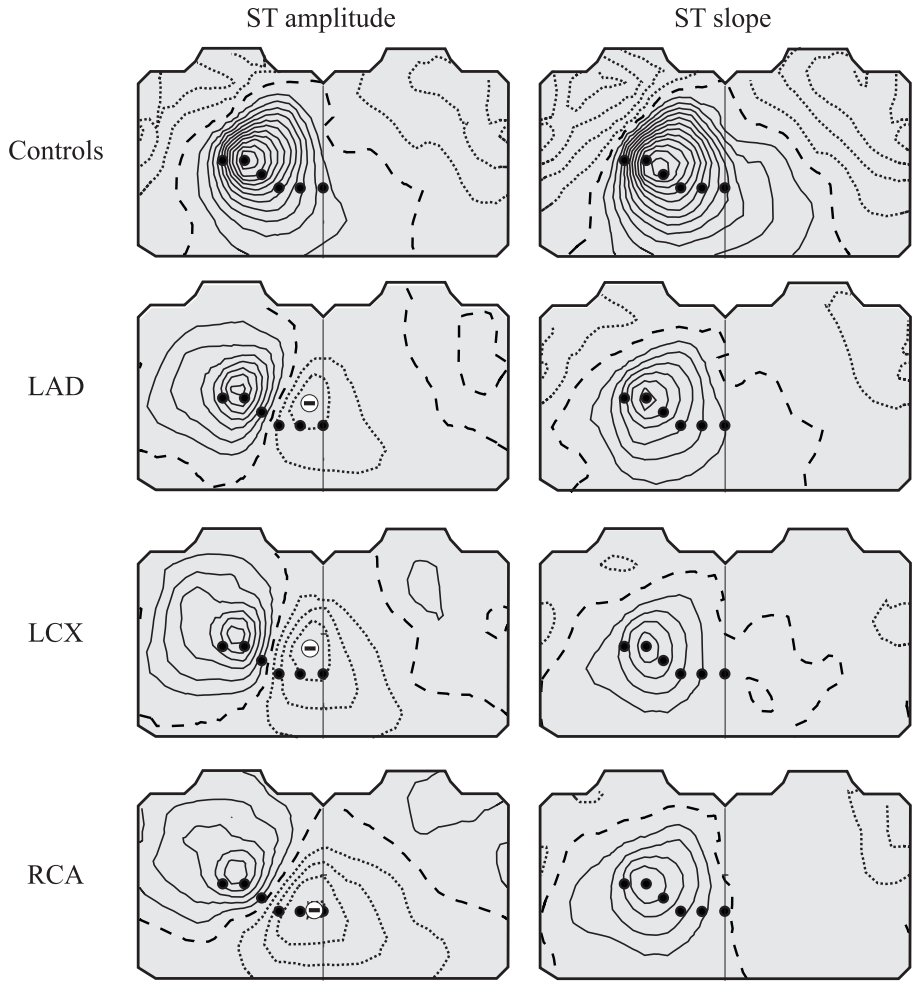

Fig. 17: *Group-mean maps of the ST amplitude (left) and ST slope (right) at cessation of exercise. Healthy controls (top) had a maximum of electric potential over the anterior chest and a depressed ST segment over the upper right thoracic area. In patients with anterior (LAD) or posterior (LCX) ischemia the maximum ST segment depression was at the lower left thorax, above electrodes V_5 and V_6 in the 12-lead ECG. The corresponding location in the patients with inferior ischemia (RCA) was between the electrode locations V_5 and V_6. The ST slope map in the controls indicated steeper ascending ST segment configuration at the lower left, and a steeper descending configuration at the upper right thorax compared to the CAD patients. The step between two isocontour lines is 25 μV in the amplitude maps and 300 $\mu V/s$ in the ST slope maps. Black dots indicate the locations of the V_1–V_6 electrodes in the 12-lead ECG. Solid isocontour lines denote positive potential or ascending slope and dotted lines denote negative potential or descending slope. (From Publication VI)*

horizontal ST slope at lower left thorax. At the upper right thoracic area the CAD patients had a higher ST segment amplitude and less descending ST slope compared to the controls.

The DI maps of the ST segment depression and the ST segment slope of the pooled CAD patient group are illustrated in Fig. 18. The optimal area for detecting ST depression or ischemia-induced decrease in the ST slope was at the lower left thorax and it was mostly

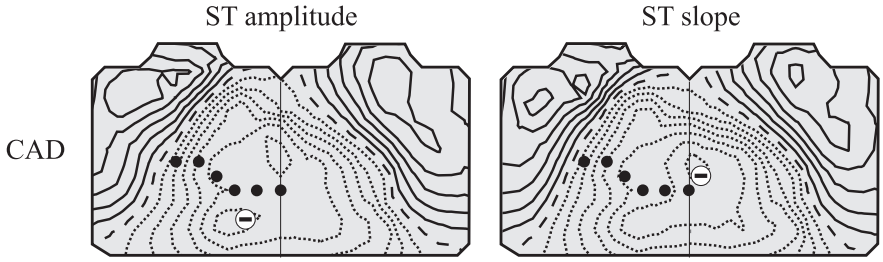

Fig. 18: *The DI maps of the ST segment amplitude and slope at cessation of exercise in the pooled CAD patient group. The step between two isocontour lines is 0.25. Solid isocontour lines denote positive, and dotted lines negative value of DI. Black dots indicate the locations of the V_1–V_6 electrodes in the 12-lead ECG. The extrema of the DI maps suggest that optimal locations for detecting ischemia-induced ST depression or ST slope decrease is at the lower left thorax. The corresponding locations for ST slope increase and ST elevation are over the upper right thoracic area. (From Publication VI)*

covered by precordial ECG leads V_4–V_6. The highest DI values, indicating ischemia-induced ST elevation and slope increase, were over the right shoulder and the upper right back. In the patient subgroups with different ischemic regions, the extrema of the DI were approximately at the same areas as in the pooled CAD group.

When the optimal leads were evaluated, the ST segment depression was more extensive in the pooled CAD group and in all patient subgroups than in the control group. The ST slope decrease due to exercise was more extensive in the CAD groups, compared to the control group. The ST slope at the lower left thorax had a higher AUC than the ST depression at the same area in the pooled CAD group (97 % vs. 93 %), and in all patient subgroups.

6 Discussion

6.1 Magnetic and electric mapping in healthy subjects

In Publication I, the exercise-induced changes of the MCG in healthy subjects during the ST segment and the T wave were quantified by calculating the alterations in the amplitude of the MFMs. An amplification of the MCG signal minimum over the mapped area took pace as a response to exercise and the monopolar difference map pattern indicated exercise-induced magnetic flux component outward the chest over the mapped area. The changes were larger in the MCG than in the BSPM. These results support the earlier findings by Brockmeier *et al.* (1994 and 1997). They found alterations of the ST segment and the T wave due to physical (Brockmeier *et al.* 1994) and pharmacological (Brockmeier *et al.* 1997) stress in the MCG, but not in the simultaneously obtained ECG. These alterations included ST segment depression, T wave inversion, and monopolar MFMs during the repolarisation period of the cardiac cycle. The authors suggested that the changes could be induced by a vortex current (Brockmeier *et al.* 1997). The results obtained in this thesis support this view.

Contrary to earlier results (Brockmeier *et al.* 1997), a significant difference was not found between the MCG and the BSPM in the correlation of maps at rest with those postexercise. This discrepancy could originate from the different MCG and BSPM measurement setups. Here, both the MCG and the BSPM covered a more extensive area compared to the previous work.

In Publication I, the lower inter-individual variation in the BSPM compared to the MCG may also have been due to differences in the mapped area, because the BSPM extended over the whole upper thorax whereas the MCG covered the frontal chest only. The variation between subjects both in the MCG maps and the BSPM maps was lowest at the T wave apex. The data of the T wave provide therefore a more reliable reference of the normal findings in the exercise MCG than the ST segment data.

Because of the changes of the ST segment amplitude in healthy volunteers in the MCG, the maximum ST segment depression over the mapped area could not be used as an indicator of ischemia. Therefore, other MCG parameters for detection of ischemia were developed in the studies on CAD patients.

6.2 Detection of ischemia by magnetocardiography

Exercise-induced ischemia occurs typically at subendocardium and causes ST segment depression in left precordial ECG leads V_4–V_6 and in inferior leads II, III, and aVF (Chaitman 1997). These changes suggest that the ischemia-induced current during the ST segment is directed roughly from the lower left to the upper right thorax, although location of the ischemic area affects the orientation. The BSPM results of this thesis indicated ST depression

at lower left thorax and ST elevation at upper right, and supported this view about the orientation of the ischemic current. The simple model, presented in section 2, suggests that such a current would result in a magnetic flux toward the upper left chest and outward the central inferior thoracic area. This flux pattern is in a reasonable concordance with the experimental results obtained in this thesis, despite the extreme simplicity of the source current and the volume conductor in the model. The most sensitive MCG recording locations for detecting exercise-induced ST segment depression and elevation, studied in Publication III and presented also in Fig. 12, suggested that the injury current generated a magnetic flux toward the upper left chest (ST elevation) and outward the central inferior thoracic area (ST depression). Similar type of alterations were found in the signal distributions at the T wave apex (Fig. 12).

An MFM observed at the ST segment during ischemia has components originating both from the normal electrical activation and from ischemic current. Superposition of the signal distribution originating from the normal activation and the distribution induced by ischemia could have caused the rotation of the MFMs during the ventricular repolarisation in CAD patients. The group mean MFMs observed in healthy volunteers during repolarisation (Figs. 7 and 8) differed considerably from the ischemia-induced alteration in CAD patient group (Fig. 12). The magnetic field originating from the ischemic current may have partially canceled the field from the normal activation and affected the orientation of the observed MFM.

In CAD patients, contribution of the ischemic injury current to the observed MFM changes upon recovery from exercise. In Publication V, the time development of the MFM orientation had a high variation between the subjects during the reversal of ischemia. Differences in the development of the extent of ischemia during the recovery, even in patients with the same stenosed vessel, are likely to have contributed to the extensive differences between the patients. In general, the intra-individual development of MFMs during the recovery was smoother in healthy controls than in the CAD patients and also the inter-individual variation was lower.

In addition to rotation of MFMs, exercise caused a tendency toward a more monopolar magnetic field pattern over the mapped area in the CAD patients, when compared to the controls. A separate parameter was not used for quantifying the degree of monopolarity of the MFMs. Monopolarity was, however, found to contribute to the MFM orientation because it resulted in abrupt changes in the orientations of MFMs in some patients during the recovery.

In Publications IV and V, a regression line was fitted in the MFM orientation vs. HR data to quantify the change in MFM orientation related to the change of the HR. In general, the dependence was not linear in the CAD patients. Nevertheless, linear regression was used but merely to quantify the change of the MFM orientation and to adjust it with the

corresponding change in the HR. Although the linear model was not wholly appropriate it was a simple way to reflect the change in the orientation of MFMs.

In Publication V, the MFM angle/HR slope was negative in three patients at the ST segment (one in each subgroup of different stenosed vessel) and in six patients at the T wave (5 LAD patients, one RCA patient). Considering the large variation between subjects in the time development of the MFM orientation at the presence of ischemia, it is difficult to assess the meaning of the direction of the MFM rotation. Therefore, only the absolute value (magnitude) of the slope was used when quantifying the change in the MFM orientation.

The beta-blockers were continued through the measurements of the CAD patients due to patient safety. The beta-blockade, lowering the HR and the degree of ischemic changes, might have been disadvantageous for the MCG ST/HR analysis. In ECG studies, evaluating the factors affecting the performance of ST/HR slope and ST/HR index in patients taking or not taking beta-blockers (Okin 1985, Kligfield 1993), the mean and peak exercise HRs were both lower in patients taking beta-blockers. However, the difference between these patient groups in overall HR change during exercise was not significant. Thus, it seems unlikely that the beta-blockade would have induced false positive ischemic responses during exercise testing.

6.3 Detection of ischemia by body surface potential mapping

One region sensitive to ischemia-induced ST segment depression and ST segment slope decrease was identified in Publication VI. Despite variation in the culprit coronary artery and presence or absence of a history of MI, the region was common for all CAD patient groups. The optimal area was relatively well covered by leads V_4–V_6 of the 12-lead ECG. The results of Publication VI also suggested that another area, at the upper right thorax, was sensitive to ischemia-induced ST segment elevation and ST segment slope increase. In the 12-lead exercise ECG setup this area is best sampled by the aVR lead. Thus, the optimal lead combination in the 12-lead ECG could be the difference of V_5, for example, and aVR. Such a derived lead could show a more depressed and a steeper down-sloping ST segment during ischemia than the standard leads.

In the MCG, the spatial signal gradient used in determining the MFM orientation had typically a distinct maximum over the mapped area in the healthy volunteers at the ST segment, and especially at the T wave apex. This resulted in relatively low inter-individual variation in the values of the MFM angle. In the BSPM, the distribution of the electric potential at the ST segment in healthy subjects had typically a strong global maximum over the chest both at rest and postexercise (Fig. 7). The spatial gradient of the potential in such a BSPM distribution has a wide circular area of almost identical values of the gradient around the location of the maximum potential. The directions of the gradient over this circle cover

all values of angle. Therefore, healthy controls might have a large inter-individual variation in the gradient angles. This, in turn, would be a disadvantage in the separation of CAD patients and healthy controls by the gradient method in the BSPM.

6.4 Clinical feasibility of stress magnetocardiography

6.4.1 Costs and performance

The recording and analysis methods developed in this thesis aimed at detection of exercise-induced ischemia. Since no additional imaging techniques were required, costs and clinical performance compared to the ECG determine the feasibility of the exercise MCG. At present, the MCG recording equipment and magnetic shielding are expensive and the exercise recordings made for research purposes are time-consuming. For clinical purposes the measurement protocol could be optimised, which would expedite the recordings. Also, the signal analysis methods presented in this thesis are not computationally demanding and the analysis could be performed on-line. In principle, the duration of an exercise MCG recording and analysis could be of the same order or lower than that of the exercise ECG recording. The analysis methods presented in this thesis are not very sensitive to noise. Therefore, with further development in the recording technology, they might be feasible also in the analysis of recordings with high temperature SQUID sensors in an unshielded environment. This would reduce costs of the recordings.

The small size of the study population of this thesis did not allow suggestion of optimal cut-off values for separating CAD patients and healthy controls by the MCG parameters. A study with a larger patient population is required to determine the normal limits for the MCG parameters. Thereafter, assessment of the performance of the exercise MCG is possible. It should be evaluated, for example, if the rate of false positive findings in female subjects is as high in the MCG as in the standard exercise ECG. In this thesis, the inclusion required the CAD patients to have a significant ST segment depression in the 12-lead exercise ECG at screening. For comparison of the performance of the MCG with the 12-lead exercise ECG used in clinical practice, also CAD patients without ST depression in the ECG would have to be studied. The standard ECG analysis utilises the data recorded during exercise and the corresponding MCG was not analysed in this thesis. However, some knowledge of the performance of the MCG compared to the 12-lead ECG was obtained in Publication V, where the MCG and the ECG recorded simultaneously during the recovery period of exercise testing were studied. The MCG showed better performance than the 12-lead ECG in detection of ischemia when both data were analysed with similar type of methods.

6.4.2 Detection of CAD by magnetocardiography at rest

In MCG recordings at rest, temporal aspects of the signal during repolarisation have been reported to differ between patients with CAD but no history of MI, and patients with chest pain but without CAD (Hailer *et al.* 1999, Van Leeuwen *et al.* 1999). The MCG analysis in this thesis was limited to MFMs, and the QT interval dispersion, for example, was not evaluated. The only indication of difference between CAD patients and controls at rest was the different ST segment MFM orientation between the RCA patient subgroup and controls in Publication II. However, the focus of this thesis was on the data recorded postexercise and differences between patients and controls at rest can not be excluded. Detection of ischemic heart disease at rest would considerably increase the clinical significance of the MCG.

6.4.3 Pharmacological stress

Clinical practice indicates preference of physical over pharmacological stress in the ECG. In general, pharmacological stress is used only when physical exercise is not possible. In the MCG, lower noise obtained with pharmacological stress is of benefit, especially if high signal to noise ratio is required. Considering the screening of ischemia and development of stress MCG as a first-line diagnostic test, physical exercise has the benefit of being non-invasive and more natural test compared to pharmacological stress.

6.4.4 On-line analysis of magnetic field map orientation

Signal processing in this thesis was performed off-line. However, the analysis method presented in Publication IV could, in principle, be applied also to an on-line analysis. Planar gradiometer units record directly the spatial derivatives of B_z and the calculation of the MFM orientation is therefore simple. In the present analysis, the calculation of the non-linear baseline estimate was the computationally most demanding operation. With a higher corner frequency of the high-pass filtering, some of the baseline drifting could be canceled without distorting the signal too extensively. Therefore, it might be possible to perform the analysis also with linear baseline estimation. Because pharmacological stress induces less noise than physical exercise, the non-linear baseline estimation might not be necessary if drugs are used to provoke ischemia.

6.5 Main limitations of this thesis

The study population of this thesis was relatively small and especially the findings on the performance of the exercise MCG in the ischemia detection should be considered preliminary. Due to technical limitations, the MCG and the BSPM were not recorded simultaneously, which would be the optimal setup for comparing the two mappings. However, the difference in the maximum HR in the two exercise mappings was not significant. The MCG analysis

was limited to data recorded postexercise in this thesis. With further experience in the exercise MCG, data suitable for analysis can also be recorded during exercise.

The supine stress may have hampered ischemia detection, partly due to lower rate-pressure product compared to upright exercise testing. In principle, also MCG devices for upright measurements could be constructed. In Publications I–V, only patients with single vessel CAD without MI were studied and ischemia detection in the presence of an old MI or multivessel CAD was not assessed. On the other hand, changes of the ST segment and the T wave due to myocardial scar did not confound the specificity to ischemia. Evaluation of ischemic regions was based on the location of a stenosis in coronary angiography. Isotope ventriculography would have further improved the evaluation of ischemic myocardial regions. Because the MCG and the BSPM recordings were performed during the same day, ischemic preconditioning may have had an effect on the second exercise test in the patients. However, the recordings were made in random order to reduce this bias.

6.6 Main findings of this thesis

In healthy volunteers, exercise was found to induce more extensive alterations in the MCG than in the BSPM during the ventricular repolarisation. Although the ST segment level is routinely evaluated in the 12-lead exercise ECG, the maximum ST segment depression over the mapped area in the MCG was not a feasible parameter for detection of ischemia. However, the physical exercise induced a rotation of the MFMs at the ST segment and the T wave in CAD patients. The MFM orientation could successfully be used as a parameter for ischemia detection. Optimal recording locations for detecting ischemia by exercise-induced amplitude change in the MCG and the BSPM were also studied. At the optimal MCG locations, also the ST segment depression was sensitive to ischemia. In the BSPM, a region sensitive to ischemia-induced ST segment depression and ST segment slope decrease was identified. The region was common for all CAD patient groups, in spite of variation in the location of ischemia and presence or absence of a history of MI.

A method for analysing beat-to-beat alterations in the MCG and the BSPM distributions at a given time interval of the cardiac cycle was developed. It enables monitoring of the MFMs, for example during recovery from physical exercise. It also makes possible studying of different parameters, calculated from the MFMs or the BSPMs, as a function of time or HR. In this thesis the method was used for quantifying exercise-induced change in the orientation of MFMs in CAD patients and healthy controls. Adjustment of the change in the orientation of MFMs with the corresponding HR change improved ischemia detection by the exercise MCG. When simultaneously recorded data at the recovery period of exercise testing were evaluated with similar type of analysis methods, the MCG showed better performance than the 12-lead ECG in ischemia detection.

Summary of Publications

I Magnetocardiographic and electrocardiographic exercise mapping in healthy subjects (*Ann. Biomed. Eng.* **29** 501–9, 2001).

The normal response to physical exercise in magnetocardiography (MCG) and body surface potential mapping (BSPM) was studied. The MCG and the BSPM were recorded in 12 healthy middle-aged subjects during supine bicycle exercise testing. The exercise-induced changes in the signals were quantified with parameters based on signal amplitude and spatial signal distribution. The main focus was on the ventricular repolarisation. At this time period, exercise was found to induce a magnetic field component outward the precordium. Also, the minimum value of the MCG signal over the mapped area at the ST segment and the T wave apex was amplified due to stress. The response to exercise was weaker in the BSPM than in the MCG. The negative component in the MCG signal over the mapped area during the repolarisation was found to be a normal physiological response to exercise. It was concluded that unlike in clinical exercise electrocardiography (ECG), the maximum ST segment depression over the mapped area in the MCG might not be an eligible parameter when evaluating the presence of ischemia by the exercise MCG.

II Detection of exercise induced myocardial ischemia by multichannel magnetocardiography in single vessel coronary artery disease (*Ann. Noninv. Electrocardiology* **5** 147–57, 2000).

The aim in this publication was to find the features of the MCG signal which are altered by exercise-induced ischemia, and to develop a parameter for quantifying them. Forty-four subjects, including 27 patients with single vessel coronary artery disease (CAD) and a control group of 17 healthy volunteers, were studied with exercise MCG and simultaneous 12-lead ECG. The principal finding was that ischemia induced a rotation of the magnetic field maps (MFMs) at the ST segment and at the T wave apex. The MFM orientations were quantified both by manual measurement, based on locations of the signal extrema, and by a new surface gradient method. Orientations of the MFMs at the ST segment in the CAD patient group differed from orientations of the control group both immediately and 4 minutes after exercise, but not at rest. The MFM orientation at the T wave apex 4 minutes postexercse was different in the CAD patient group compared to the control group. The T wave analysis performed better 4 minutes postexercise than at cessation of exercise. Orientation of the MFM at the ST segment and at the T wave was concluded to be sensitive to transient ischemia.

III Recording locations in multichannel magnetocardiography and body surface potential mapping sensitive for regional exercise-induced myocardial ischemia (*Basic Res. Cardiol.* **96** 405–14, 2001).

This study aimed at identifying the optimal recording locations in the MCG and the BSPM for detection of exercise-induced ischemia. Study group comprised 24 CAD patients with single vessel disease and 17 healthy volunteers. The optimal locations for detecting ischemia-induced alteration in the amplitude of the ST segment and T wave were identified by calculating discriminant index (DI) maps for both time intervals in the MCG and the BSPM. In the BSPM, the optimal recording location for separating CAD patients from controls by the ST segment depression at cessation of exercise was at the lower left side, below the lead V_5 of the 12-lead ECG. The optimal area for detecting ischemia-induced ST segment elevation was over the upper right anterior and posterior thorax. In the MCG, the optimal locations for detecting ischemia by the ST segment depression were over the central inferior part of the chest. The corresponding locations for the ST elevation were over the upper left part of the thorax. In the optimal MCG and BSPM measurement locations, the parameters studied (ST segment depression and elevation, T wave amplitude increase and decrease) were significantly different in the CAD patient group, compared to the control group.

IV Beat-to-beat analysis method for magnetocardiographic recordings during interventions (*Phys. Med. Biol.* **46** 975–82, 2001).

A method for beat-to-beat analysis of MCG data was developed in this study. The method enabled extraction of MFMs at a given time instant from each cardiac cycle during recovery from exercise, and monitoring of their development. Signal to noise ratio of the MFMs was improved by mean filtering. In this manner, blurring of the signals during ventricular repolarisation, observed in conventional signal averaging, was avoided. A method for quantifying the exercise-induced change in the MFM orientation and adjusting it with the corresponding alteration in the heart rate (HR) was also developed. The analysis methods were tested with exercise MCG data, recorded in three CAD patients and two healthy volunteers. The HR adjusted MFM rotation during recovery period of exercise testing was more extensive in the patients compared to the controls. The analysis method presented in this study can be applied also to an on-line processing of MCG data. In addition, the method for extracting spatial signal distributions can be applied to analysis of other bioelectromagnetic signals, such as BSPM.

V Heart rate adjustment of magnetic field map rotation in detection of myocardial ischemia in exercise magnetocardiography (*Basic Res. Cardiol.* Accepted for publication, 2001).

The analysis method developed in Publication IV was applied to exercise MCG data recorded in 24 patients with single vessel CAD and 17 healthy volunteers. The aim was to evaluate the performance of HR adjusted change in the MFM orientation in detection of exercise-induced ischemia. The results were compared to the un-adjusted MFM orientation, and to the 12-lead ECG both with and without HR adjustment. During the recovery period of exercise testing, the HR adjusted MFM rotation was more extensive in the CAD patient group than in the control group. The HR adjusted MFM rotation at the ST segment performed better than the un-adjusted MFM orientation at the ST segment immediately after exercise. It also had a higher or equal sensitivity to CAD, when compared to the HR adjusted ST segment depression in the ECG, at all values of specificity. At the T wave, the HR adjusted MFM rotation had an equal or higher sensitivity compared to the MFM orientation 4 minutes postexercise, independent of the required specificity. The MCG was found to be superior to the 12-lead ECG in detection of ischemia, when data recorded postexercise were evaluated.

VI ST segment level and slope in exercise-induced myocardial ischemia evaluated with body surface potential mapping (*Am. J. Cardiol.* Accepted for publication, 2001).

BSPM was recorded during exercise testing in 25 healthy controls, 27 single vessel CAD patients, and in 18 patients with triple vessel CAD and a history of one or more myocardial infarcts (MIs). The aim was to study the performance and optimal recording locations of the ST segment slope in detection of exercise-induced ischemia. The patients were classified into three subgroups, according to the main ischemia region. DI maps of ischemia-induced alteration in ST segment amplitude and slope were calculated for all patient groups. The leads with the highest absolute DI value were considered optimal. The optimal area for detecting ST depression or ischemia-induced decrease of ST slope were at the lower left thorax in the pooled CAD patient group. In the patient subgroups with a different ischemic region, the extrema of the DIs were approximately at the same areas as in the pooled CAD group. In the optimal leads, the ST slope decrease as well as the ST depression due to exercise were more extensive in all patient groups, when compared to the control group. One region, sensitive for ischemia-induced ST segment depression and ST segment slope decrease, was identified. The region was common for all CAD patient groups, despite variation in the location of ischemia and presence or absence of a history of MI.

Statement of involvement

All publications included in this thesis are results of a group effort. The author of this thesis designed and constructed the non-magnetic exercise ergometer which was used in the measurements in all publications. The author was also responsible for the technical development needed for implementing the protocol for the exercise MCG measurements. The signal analysis in Publication I was performed by the author. The author played a significant role in finding the signal averaging method for exercise MCG and BSPM signals used in Publications I–III and VI. The extraction of the data of interest in these publications, and calculation the ST segment slopes in Publication VI were performed by the author. The author had a significant contribution to the innovation and development of parameters used for quantifying the ischemia-induced alterations in the MCG and the BSPM in Publications II–VI. The author developed the beat-to-beat analysis method described in Publication IV and utilised in Publication V. The author also performed the signal analysis in both of these publications. The author wrote publications I, IV, and V, and participated in writing of the other publications.

Acknowledgments

The work for this thesis was accomplished at the Laboratory of Biomedical Engineering at Helsinki University of Technology and at the BioMag Laboratory of Helsinki University Central Hospital. I thank the supervisor of this thesis, Professor Toivo Katila, Dr.Tech., for his contribution in drawing together excellent research facilities and an inspiring research group. My instructor, Juha Montonen, Dr.Tech., I wish to thank for his invaluable guidance which started long before the work presented in this thesis.

I thank Helena Hänninen, M.D., for her contribution to the patient measurements, the data analysis, and the reporting of the results during the work for this thesis. I am grateful for her decisiveness and commitment to research work, and for the fruitful and intensive co-operation, which made possible completion of this thesis.

I owe warmest thanks to all colleagues working at the Laboratory of Biomedical Engineering for an enjoyable and stimulating working environment. Especially, I wish to thank Jukka Nenonen, Dr.Tech., for his ideas and work on the data analysis programs. The contribution of Kim Simelius, Lic.Sc., to the development of the body surface potential mapping system was of vital importance for accomplishing this thesis, and I wish to express my gratitude to him. I thank Katja Pesola, Dr.Tech., for the enjoyable years of working together in the laboratory. I am very grateful to the Head of the BioMag Laboratory, Docent Risto Ilmoniemi, Dr.Tech., for the excellent measurement facilities.

I am deeply indebted to Docent Lauri Toivonen, M.D., for his research ideas, and thorough and innovative review of manuscripts. I wish to express my thanks to Docent Markku Mäkijärvi, M.D., for his contribution to bringing together the interdisciplinary research group and establishing international collaboration. I am grateful to Petri Korhonen, M.D., and Lasse Oikarinen, M.D., Ph.D., for their effort in making the patient measurements.

I give my warmest thanks to my beloved wife Tiina for her love, and for being such as she is. My parents, Pekka and Tuulikki I wish to thank for their continuous support throughout my life.

I express my gratitude to Docent Pekka Raatikainen, M.D., and Professor Gerhard Stroink, Ph.D., for reviewing the manuscript of this thesis. The financial support of the Academy of Finland, the Jenny and Antti Wihuri Foundation, and the Foundation of technology in Finland is gratefully acknowledged.

Espoo, October 23, 2001

Panu Takala

References

Alexander K P, Shaw L J, Delong E R, Mark D B, Peterson E D Value of exercise treadmill testing in women *JACC* **32**(6) 1657–64 (1998).

Baule G and McFee Detection of the magnetic field of the heart *Am Heart J* **55** 95–8 (1963).

Brockmeier K, Comani S, Erne S N, Di Luzio A, Pasquarelli A, Romani G L Magnetocardiography and exercise testing *J Electrocardiol* **27** 137–42 (1994).

Brockmeier K, Schmitz L, Chavez J, Burghoff M, Koch H, Zimmerman R, Trahms L Magnetocardiography and 32-lead potential mapping: Repolarization in normal subjects during pharmacologically induced stress *J Cardiovasc Electrophysiol* **8** 615–26 (1997).

Brockmeier K, Van Leeuwen P Magnetocardiographic stress test investigations analyzing ventricular repolarization changes *Biomag2000, Proc. 12th Int. Conf. on Biomagnetism* Nenonen J, Ilmoniemi R J, Katila T, (eds). Helsinki Univ. of Technology, Espoo, Finland pp. 546–48 (2001).

Chaitman B Exercise testing. *Heart disease A textbook of cardiovascular medicine* Braunwald E (ed) W.B. Saunders Company, Philadelphia pp. 153–76 (1997).

Cohen D, Lepeschkin E, Hosaka H, Massell B F, Myers G Abnormal patterns and physiological variations in magnetocardiograms *J Electrocardiol* **9** 398–409 (1976).

Cohen D and Hosaka H Magnetic field produced by a current dipole *J Electrocardiol* **9** 409–17 (1976b).

Cohen D, Savard P, Rifkin R, Lepeschkin E, Strauss W E Magnetic measurement of S-T and T-Q segment shifts in Humans. Part II: Exercise-induced S-T segment depression. *Circ Res* **53** 274–279 (1983).

Fischer G, Haueisen J, Tilg B Modre R, Wach P, Nowak H, Schwarz G, Leder U On T-wave inversion observed in magnetocardiographic stress recordings – Analysis of simulated and measured data *Biomag2000, Proc. 12th Int. Conf. on Biomagnetism* Nenonen J, Ilmoniemi RJ, Katila T, (eds). Helsinki Univ. of Technology, Espoo, Finland pp. 549–52 (2001).

Fletcher G F, Balady G, Froelicher V F, Hartley L H, Haskell W L, Pollock ML Exercise standards. A statement for healthcare professionals from the American Heart Association *Circulation* **91** 580–615 (1995).

Fridericia L Systolendauer im electrocardiogramm bei normalen menschen und bei herzkranken *Acta Med Scand* **53** 469–86 (1920).

Gianrossi R, Detrano R, Mulvihill D, Lehman K, Dubach P, Colombo A, McArthur D, Froelicher V Exercise-induced ST depression in the diagnosis of coronary artery disease: A meata-analysis *Circulation* **80** 87–98 (1989).

Gessner C, Endt P, Burghoff M, Trahms L Vortex currents detected by stress MCG and fragmentation of ECG/MCG in VT patients *Biogybernetics and Biomedical Engineering* **19** 39–51 (1999).

Hailer B, Van Leeuwen P, Lange S, Wehr M Spatial distribution of QT dispersion measured by magnetocardiography under stress in coronary artery disease *J Electrocardiol* **32** 207–16 (1999).

Hänninen H, Takala P, Mäkijärvi M, Montonen J, Nenonen J, Katila T, Toivonen L Detection of Exercise Induced Myocardial Ischemia by Multichannel Magnetocardiography in Patients with Single Vessel Coronary Artery Disease *Recent Advances in Biomagnetism: Proceedings of the 11th International Conference on Biomagnetism* Yoshimoto T, Kotani M, Kuriki S, Karibe H, and Nakasato N (eds). Tohoku University Press, Sendai pp. 1037–1040 (1999).

Kandori A, Kanzaki H, Miyatake K, Hashimoto S, Itoh S, Tanaka N, Miyashita T, Tsukada K A

method for detecting myocardial abnormality by using a total current-vector calculated from ST-segment deviation of a magnetocardiogram signal *Med Biol Eng Comput* **39** 21–8 (2001).

Kandori A, Kanzaki H, Miyatake K, Hashimoto S, Itoh S, Tanaka N, Miyashita T, Tsukada K A method for detecting myocardial abnormality by using a current-ratio map calculated from an exercise-induced magnetocardiogram *Med Biol Eng Comput* **39** 29–34 (2001b).

Kawaoka P Y and Yamashiro S M Separation of cardiac conduction system and atrial activities by spatial regression *Med Eng Phys* **18** 45–50 (1996).

Kligfield P, Ameisen O, Okin P Heart rate adjustment of ST segment depression for improved detection of coronary artery disease. *Circulation* **79** 245–55 (1989).

Kligfield P, Okin P M, Goldberg H L Value and limitations of heart rate-adjusted ST segment depression criteria for the identification of anatomically severe coronary obstruction: Test performance in relation to method of rate correction, definition of extent of disease, and β-blocade. *Am Heart J* **125** 1262–1268 (1993).

Kornreich F, Montague T J, Rautaharju P M Identification of first acute Q wave and non-Q wave myocardial infarction by multivariate analysis of body surface potential maps. *Circulation* **84** 2442–53 (1991).

Lant J, Stroink G, ten Voorde B, Horacek B M, Montague T J Complementary nature of electrocardiographic and magnetocardiographic data in patients with ischemic heart disease. *J Electrocardiol* **23** 315–22 (1990).

McPherson D D, Horacek B M, Sutherland D J, Armstrong C S, Spencer C A, Montague T J Exercise electrocardiographic mapping in normal subjects. *J Electrocardiol* **18** 351–60 (1985).

Meyer C and Keiser H Electrocardiogram baseline noise estimation and removal using cubic splines and state-space computation techniques. *Computers and Biomedical Research* **10** 459–470 (1977).

Montonen J, Ahonen A, Hämäläinen M, Ilmoniemi R J, Laine P, Nenonen J, Paavola M, Simelius K, Simola J, Katila T Magnetocardiographic functional imaging studies in the BioMag laboratory *Biomag 96, Proceedings of the tenth international conference on biomagnetism* Aine C J, Okada Y, Stroink G, Swithenby S J, Woods C C (eds). Springer-Verlag, New York pp. 494–7 (2000).

Moshage W and Achenbach S Clinically significant differences between ECG and MCG. *Biomedizinische Technik* **42**(S1) 25–7 (1997).

Mäkijärvi M, Hänninen H, Takala P, Pesola K, Nenonen J, Lauerma K, Montonen J, Korhonen P, Oikarinen L, Toivonen L, Katila T Detection and Localization of Myocardial Ischemia and Viability by Magnetocardiography *Recent Advances in Biomagnetism: Proceedings of the 11th International Conference on Biomagnetism* Yoshimoto T, Kotani M, Kuriki S, Karibe H, Nakasato N (eds). Tohoku University Press, Sendai pp. 998–1001 (1999).

Nowak H Biomagnetic instrumentation *Magnetism in medicine* W Andrä and H Nowak (eds). Wiley-VCH, Berlin pp. 88–135 (1998).

Okin P M, Kligfield P, Ameisen O, Goldberg H L, Borer J S Improved accuracy of the exercise electrocardiogram: identification of three-vessel coronary disease in stable angina pectoris by analysis of peak rate-related changes in ST segments. *Am J Cardiol* **55** 271–276 (1985)

Okin P and Kligfield P Heart rate adjustment of ST segment depression and performance of the exercise electrocardiogram: a critical evaluation. *J Am Coll Cardiol* **25** 1726–1735 (1995).

Pesola K, Hänninen H, Lauerma K, Lötjönen J, Mäkijärvi M, Nenonen J, Takala P, Voipio-Pulkki L-M, Toivonen L, Katila T Current density estimation on the left ventricular epicardium: A potential method for ischemia localization *Biomedizinische Technik* **44** (suppl. 2) 143–146

(1999).

Paavola M, Ilmoniemi R, Sohlström L, Meinander T, Penttinen A, Katila T High performance magnetically shielded room for clinical measurements *Biomag 96, Proceedings of the tenth international conference on biomagnetism* Aine CJ, Okada Y, Stroink G, Swithenby SJ, Woods CC (eds). Springer-Verlag, New York pp. 87–90 (2000).

Paavola M, Simelius K, Montonen J, Nenonen J, Katila T Averaging in Cardiographic Signal Processing *Finnish signal processing symposium, Finsig'95, symposium proceedings*, Espoo: TKK Offset, pp. 138–141 (1995).

Saarinen M, Karp P, Katila T, Siltanen P The magnetocardiogram in cardiac disorders. *Cardiovasc Res* **8** 820–34 (1974).

Savard P, Cohen D, Lepeschkin E, Cuffin B N, Madias J E Magnetic measurement of S-T and T-Q segment shifts in Humans Part I: Early repolarization and left bundle branch block. *Circ Res* **53** 264–73 (1983).

Seese B, Moshage W, Achenbach S, Killmann R, Bachmann K Magnetocardiographic (MCG) analysis of myocardial injury currents *Biomagnetism: Fundamental research and clinical applications*, Amsterdam:Elsevier/IOS-Press, pp. 628–632 (1995).

Surawicz B Electrophysiologic basis of ECG and cardiac arrhythmias. Williams & Wilkins, Malvern, PA, USA (1995).

Takala P Exercise ergometer in cardiomagnetic measurements. Master's thesis, Helsinki University of Technology. In Finnish (1997).

Takala P, Hänninen H, Montonen J, Mäkijärvi M, Nenonen J, Oikarinen L, Simelius K, Toivonen L, Katila T Comparison of Magnetocardiographic and Electrocardiographic Exercise Mapping in Healthy Volunteers *Recent Advances in Biomagnetism: Proceedings of the 11th International Conference on Biomagnetism* Yoshimoto T, Kotani M, Kuriki S, Karibe H, Nakasato N (eds). Tohoku University Press, Sendai pp. 306–309 (1999).

Takala P, Haapalahti P, Montonen J, Mäkijärvi M, Salorinne Y, Toivonen L, Katila T Beat-to-beat variability of T-wave in multichannel magnetocardiogram and 12-lead electrocardiogram during physiological interventions *Biomag2000, Proc. 12th Int. Conf. on Biomagnetism* Nenonen J, Ilmoniemi R J, Katila T, (eds). Helsinki Univ. of Technology, Espoo, Finland pp. 538–41 (2001).

Tripp J H Physical consepts and mathematical models *Biomagnetism, an interdisciplinary approach* Williamson SJ, Romani G-L, Kaufman L, Modena I (eds). Plenum press, New York pp. 101–39 (1982).

Tsukada K, Miyashita T, Kandori A, Mitsui T, Terada Y, Sato M, Shiono J, Horigome H, Yamada S, Yamaguchi I An iso-integral mapping tehcnique using magnetocardiogram, and its possible use for diagnosis of ischemic heart disease. *Int J Card Imaging* **16** 55–66 (2000).

Van Leeuwen P, Hailer B, Lange S, Donker D, Grönemeyer D Spatial and temporal changes during the QT-interval in the magnetic field of patients with coronary artery disease *Biomedizinische Technik* **44** (suppl. 2) 139–42 (1999).

Van Leeuwen P, Stroink G, Hailer B, Adams A, Lange S, Grönemeyer D. Rest and stress magnetocardiography in coronary artery disease. *Med Biol Eng Comput* **37** 1482–3 (1999b).

Van Leeuwen P, Hailer B, Klein A, Lukat M, Enke R, Lux R, Grönemeyer D Electric and magnetic QT iso-integral maps in patients with and without coronary artery disease under pharmacologically induced stress *Biomag2000, Proc. 12th Int. Conf. on Biomagnetism* Nenonen J, Ilmoniemi RJ, Katila T, (eds). Helsinki Univ. of Technology, Espoo, Finland pp. 557–60 (2001).

Väänänen H, Korhonen P, Montonen J, Mäkijärvi M, Nenonen J, Oikarinen L, Simelius K, Toivo-

nen L, Katila T Non-invasive arrhythmia risk evaluation in clinical environment. *Herzschr. Elektrophys.* **11** 229–34, (2000).

Winklmaier M, Achenbach S, Trahms L, Pohle C, Daniel W C, Moshage W Bicycle stress in healthy subjects: differences between ECG and biplane MCG *Med Biol Eng Comput* **37** 1478–9 (1999).